2009

Circuit Dynamics of Adult Visual Cortex

Homare Yamahachi

CIRCUIT DYNAMICS OF ADULT VISUAL CORTEX

A Thesis Presented to the Faculty of

The Rockefeller University

in Partial Fulfillment of the Requirements for

the degree of Doctor of Philosophy

by

Homare Yamahachi

June 2009

CIRCUIT DYNAMICS OF ADULT VISUAL CORTEX

Homare Yamahachi, Ph.D.

The Rockefeller University 2009

Learning and other forms of plasticity result from changes in transmission at existing synapses or the construction or elimination of synapses. Synapses occur at the juxtaposition of boutons, with their postsynaptic partners, dendrites and cell bodies. It has been assumed that connections in the primary visual cortex (V1) become static after the critical period. Recent studies show, however, that dendritic spines appear and disappear during adulthood in the normal brain. Our first objective was then to determine whether axonal branches and boutons also undergo morphological changes. To do so, we performed longitudinal studies of virally labeled neurons and their processes. An adeno-associated virus bearing the gene for enhanced green fluorescent protein (AAV.EGFP) provided long-term labeling of axons and their boutons in adult Macaque V1. To image the neurons *in vivo*, a custom-designed two-photon microscope and viewing chamber provided repeated imaging of selected locations. We examined the same EGFP-labeled axonal arbors at several

time points over periods of weeks in the adult normal cortex. We found that axons are dynamic entities, in which a subset of boutons appeared and disappeared over time, and that though axonal length and branching was largely stable, a small subset of terminals underwent elongation, retraction or appeared *de novo*. These results suggest an ongoing process of synaptogenesis and synapse elimination in adult V1. To further investigate structural plasticity in the adult V1, we studied the cortical reorganization that accompanies retinal lesions. Removal of visual input cause axonal sprouting of long-range horizontal connections from pyramidal cells in layer 2/3. Our *in vivo* approach allowed us to determine the dynamics of the process of sprouting. Immediately following retinal lesions, there was a remarkable rise in axonal density. In the following weeks, the massive increase in axon collaterals was accompanied by a comparable rate of axonal elimination. Also, boutons increased their rate of appearance and elimination beyond the rates seen in normal cortex. These data indicate that the initial sprouting of axons followed by the subsequent refinement, may account for the dynamics of receptive field changes observed during the course of topographic reorganization of visual cortex.

A mi mama que me bancó en todo para que pueda estudiar, a mi viejo que está siempre presente, y a mis hermanos, Javy y Manu, por romperse el lomo para seguir adelante.

ACKNOWLEDGMENTS

Thank you Charles for supporting me in every way.

To Dan and Wu for sharing with me your knowledge.

To Winfried for all your help.

To Justin, Sally, John, and Neta for valuable discussions about life and beyond.

To, Masaharu, Jiabin, Doruk, Nirmala, Valentin and Jennifer for always being there with an open hand.

To the techs, Tina, Keith, Travis, Pryia and Matt.

To CBC, without your support this could not be done.

To Eva.

To my friends, wherever you are and to you Brioche and Lurpak!!!

TABLE OF CONTENTS

LIST OF FIGURES

1 INTRODUCTION

1.1 PLASTICITY IN THE BRAIN

The nervous system shows considerable plasticity, allowing animals to adapt to changing internal and external environments. Plasticity occurs at all levels, from variations in the properties of single ion channels to a rewiring of large circuits; and over timescales ranging from milliseconds to years. In particular, development of the primary visual cortex (V1) is strongly influenced by visual experience during a restricted period of postnatal development called the critical period (Hubel and Wiesel, 1970; Hubel et al., 1977; Shatz and Stryker, 1978; Levay et al., 1980). During this period, experience can produce permanent and extensive modifications of cortical organization. Most of the evidence comes from studies of sensory deprivation in early postnatal development, leading to the expectation that all connections and functional properties would be fixed after this period. However, it is now evident that a large range of properties can be changed throughout life in an experience-dependent fashion. These changes have been widely observed in the adult somatosensory, auditory, motor and visual cortex (Kalaska and Pomeranz, 1979; Merzenich, Kaas, Wall, Nelson et al.,

1983; Merzenich, Kaas, Wall, Sur et al., 1983; Merzenich et al., 1984; Robertson and Irvine, 1989; Gilbert et al., 1990; Kaas et al., 1990; Heinen and Skavenski, 1991; Pons et al., 1991; Rajan et al., 1993; Gilbert, 1998). Several experiments based on fixed brain preparations demonstrate that new synapses are formed in sensory cortex after behavioral enrichment and sensory stimulation (Volkmar and Greenough, 1972; Chang and Greenough, 1982; Turner and Greenough, 1985; Knott et al., 2002). Recent developments in *in vivo* imaging allow the study of individualized neuronal structures over long periods of time in the same animal. Remarkably, in the adult somatosensory system, dendritic spines appear and disappear even in the absence of experiential manipulation (Grutzendler et al., 2002; Trachtenberg et al., 2002). However, it is unclear whether the morphological changes are restricted only to postsynaptic specializations such as spines. We therefore decided to determine whether axons can also undergo structural changes in the normal adult cortex. Furthermore, the accumulating evidence from studies on adult cortical plasticity suggests the involvement of specific components of cortical circuits, notably long-range horizontal connections from pyramidal neurons in layer 2/3 (Gilbert and Wiesel, 1979; Rockland and Lund, 1982; Gilbert and Wiesel, 1983;

Rockland and Lund, 1983; Martin and Whitteridge, 1984). These connections are likely to be involved in the recovery of functional reorganization after alterations of visual input, matching the extent of the area of reorganization (Gilbert and Wiesel, 1979) and undergoing sprouting and synaptogenesis after long periods (on the order of a year) (Darian-Smith and Gilbert, 1994). By performing *in vivo* imaging in the adult brain we can determine the dynamics of how the process of sprouting takes place. In particular we focused our attention to V1 since its circuitry, functional architecture and receptive field (RF) structure are well understood and can be accessibly studied.

1.2 RECEPTIVE FIELDS AND CORTICAL CIRCUITS

Traditionally, the RF of a neuron is defined as the area of visual field within which visual stimulation influences neural responses. The RF is further described by the properties of the sensory stimuli that most effectively drive the neuron (i.e. color, orientation) (Hubel and Wiesel, 1962; 1968; 1977). As we move from sensory receptors of the eye to

neurons in higher cortical areas, RFs become more complex, responding to combinations of stimulus features.

The main source of bottom up inputs to layer 2/3 pyramidal neurons are from neurons in cortical layer 4, which receive inputs from the lateral geniculate nucleus (LGN) (Fig. 1.1). These interlaminar connections run perpendicular to the cortical surface and represent feed-forward mechanisms. Most of the projections from layers 4 to 2/3 originate from spiny stellate neurons that utilize glutamate as their transmitter and exert an excitatory influence on their target neurons, while a smaller fraction of these feed-forward inputs arise from smooth dendritic GABAergic neurons (Somogyi et al., 1983; Anderson et al., 1994).

In contrast, horizontal connections from pyramidal neurons in layer 2/3 that run parallel to the cortical surface and extend for several millimeters across the cortical surface seem well suited for supplying modulatory inputs from more distant regions of visual space, giving cells sensitivity to the global context within which local features are presented (Gilbert and Wiesel,

1979; 1989; Mcguire et al., 1991; Keller and Asanuma, 1993; Bosking et al., 1997).

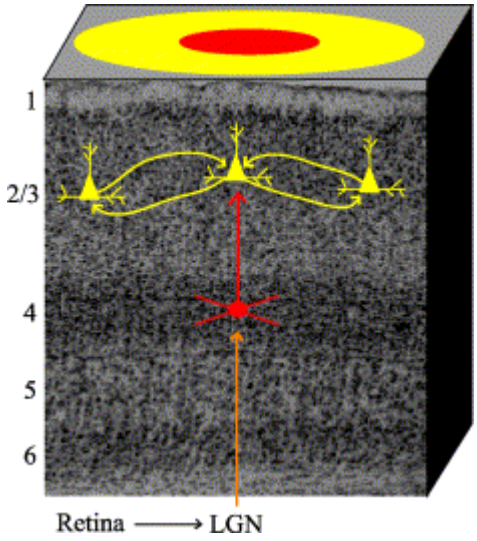

Figure 1.1: Elements of the cortical circuit in primary visual cortex

A Nissl stained histological section through primary visual cortex shows the cortical layers. The schematic overlay depicts the flow of visual information through primary feed-forward and recurrent pathways to a layer 2/3 neuron (central, yellow cell). The feed-forward pathway travels from the retina, to the lateral geniculate nucleus in the thalamus (LGN), to cortical layer 4 (red cell), and on to layer 2/3. This pathway has often been credited with establishing the response properties of the RF center (depicted in red above the cortical section). Recurrent, or horizontal, connections between layer 2/3 neurons (flanking yellow cells) have been thought of as the source for the contextual effects of the RF surround (yellow annulus above) (Rockland and Lund, 1982; Mcguire et al., 1991; Bosking et al., 1997). (Figure adapted from Chisum and Fitzpatrick, 2004)

In vitro experiments have shown that layer 4 inputs reliably evoke excitatory postsynaptic potentials (EPSPs) in layer 2/3 (Feldmeyer et al., 2002) and that these EPSPs are larger and less variable than those evoked by inputs from other layer 2/3 neurons (Hirsch and Gilbert, 1991; Yoshimura et al., 2000). Furthermore, stimulation of layer 4 inputs is more likely to drive a neuron to fire action potentials than stimulation of long-range horizontal connections (Hirsch and Gilbert, 1991). Even when using stimuli designed to elicit high levels of activity in the horizontal network, horizontal connections are insufficient to evoke detectable signals in layer 2/3 neurons unless accompanied by activation of layer 4 inputs (Chisum et al., 2003). The interlaminar connections may therefore mediate responses to stimuli placed within the RF centre, whereas the horizontal connections play a modulatory role and can account for response selectivity to more complex stimuli.

The bulk of the horizontal connections within layer 2/3 arise from pyramidal neurons (Gilbert and Wiesel, 1979; 1983; Mcguire et al., 1991; Keller and Asanuma, 1993; Bosking et al., 1997). Unlike the inputs from layer 4, horizontal connections are strongly recurrent, forming a network of

reciprocal connections between individual participants. While the majority of these connections are excitatory, there is at least one class of smooth dendritic GABAergic neuron (basket cell) that contributes to horizontal connections in layer 2/3 (Martin et al., 1983; Kisvarday and Eysel, 1993). However, these do not spread as widely (up to 2 mm) compared with the 8 mm extent of the horizontal connections from pyramidal neurons. The targets of the pyramidal cells forming the long horizontal connections include both other pyramidal cells and inhibiting interneurons, thus allowing the horizontal connections to have both facilitatory and inhibitory influences (Mcguire et al., 1991). In addition, horizontal connections terminate in a patchy fashion, targeting regions of the cortex with similar orientation preference (Stettler et al., 2002).

1.3 PERCEPTUAL LEARNING

The characteristics of intrinsic, long-range horizontal connections make them well suited to participate in a variety of perceptual discrimination tasks including contour integration (Gilbert and Wiesel, 1989; Kapadia et al., 1995; Gilbert et al., 1996; Li and Gilbert, 2002; Stettler et al., 2002) and the

extraction of texture and shading flow (Ben-Shahar et al., 2003). For instance, the ability to detect a contour of evenly spaced colinear segments embedded in a complex background is dependent upon the distance between them and can be improved upon training. Separating the segments beyond a critical distance makes the contour no longer salient. This distance correlates with the spatial extent of horizontal connections between V1 neurons (Kapadia et al., 1995; Kapadia et al., 2000; Li and Gilbert, 2002). This form of learning accomplished by repeated practice at a discrimination task is known as perceptual learning. The improvement is long lasting (weeks, months or even years) and specific to the stimulus being presented, with very little transfer to similar tasks (Gilbert et al., 2001). All sensory modalities are capable of improving their discrimination threshold with training. Monkeys trained to discriminate small differences in tonal frequency showed an increase in their performance after several weeks of training (Recanzone et al., 1993). This improvement is correlated with an expansion of the representation of the frequencies used in the task in the primary auditory cortex. In the visual system, several stimulus properties can be improved by training, such as spatial resolution (Mckee and Westheimer, 1978; Poggio et al., 1992; Crist et al., 1997), orientation

(Vogels and Orban, 1985; Shiu and Pashler, 1992), texture (Karni and Sagi, 1991) and depth (Ramachandran and Braddick, 1973; Fendick and Westheimer, 1983). This learning is retinotopic specific with little transfer to other regions of the visual field (Karni and Sagi, 1991; Sigman and Gilbert, 2000), suggesting that early on in the visual pathway, the information is stored. V1 is a possible candidate to be the repository of this information, since eye specificity, orientation and location information are mapped with highest resolution. Also, V1 circuitry components are known to be plastic, during CNS lesions (Rose et al., 1960; Kaas et al., 1990; Heinen and Skavenski, 1991; Gilbert and Wiesel, 1992; Darian-Smith and Gilbert, 1994; Keck et al., 2008), perceptual learning (Gilbert and Wiesel, 1990; Roelfsema et al., 1998; Ito and Gilbert, 1999; Schoups et al., 2001; Li et al., 2004; 2006), and even without any experiential manipulation (Holtmaat et al., 2005; De Paola et al., 2006; Majewska et al., 2006; Stettler et al., 2006). *In vivo* imaging experiments show that the stability of spines in V1 gradually increases during development and into adulthood (Holtmaat et al., 2005), but still a third of the spines in adult mice remained transient. Moreover, modification of sensory experience drives the rate by which synapses are remodeled. One advantage of this malleability is that by

having labile synapses, the CNS could adapt rapidly to changes in external and internal environments. However, if the synapses are continuously being formed and dismantled in V1, how could the information be stored so precisely regarding retinotopic space for years? Is the memory retained using only those persistent synapses?

1.4 LESION-INDUCED PLASTICITY OF SENSORY AND MOTOR MAPS

The same mutability of receptive field properties that is associated with perceptual learning is engaged in recovery of function following CNS lesions. A useful model to investigate how experience-dependent plasticity takes place in V1 is by altering visual input by making lesions in the retina, which causes changes in the physiological properties of neurons in the adult brain. For instance, lesions placed in homologous positions in the two eyes to remove visual input altered neuronal firing properties from the corresponding area of V1 (Gilbert et al., 1990; Kaas et al., 1990; Heinen and Skavenski, 1991; Darian-Smith and Gilbert, 1994; Chino et al., 1995; Darian-Smith and Gilbert, 1995; Schmid et al., 1996; Chino, 1999; Dreher et

al., 2001). By recording from identical cortical sites, using the vasculature as reference, one can follow the effect of the lesion from minutes to months after the lesioning procedure. In V1, the zone receiving input from the lesioned part of the retina is initially silenced, but over a period of a few months, it recovers visually driven activity. This area is referred to as the lesion projecting zone (LPZ). The RFs of cells in the LPZ shift from representing the lesioned part of the retina to representing the retinal area surrounding the lesion. This remapping of the cortical topography causes shrinkage of the representation of the retinal lesion and an expansion of the surrounding non-lesioned part of the retina. This reorganization may be the basis of the recovery of visual perception. The gray patch one initially sees in the part of the visual field covered by the lesion disappears, such that contours passing through the retinal scotoma will appear complete, albeit somewhat distorted (Craik, 1966; Gerrits and Timmerman, 1969; Schuchard, 1993; 1995; Burke, 1999; Zur and Ullman, 2003).

The substrate for the functional reorganization was explored by recording at various stages along the visual pathway. Although a small amount of reorganization may occur in the LGN (Eysel et al., 1980; 1981),

even when the cortex has completely reorganized, there is still a large area of LGN that remains silent, indicating that most of the reorganization must be intrinsic to the cortex (Gilbert and Wiesel, 1992; Darian-Smith and Gilbert, 1995). Moreover, the thalamic afferents cannot account for the reorganization. The extent of reorganization, ~6-8 mm in diameter, could not be explained by the lateral spread of thalamic afferents, which spread ~1.5-2 mm laterally in cortex, unless they increased their projection pattern into the center of the reorganized region. Not only are they too restricted in their normal extent, but they do not sprout into the LPZ, as would be required if they were to be responsible for the reorganization (Gilbert and Wiesel, 1992; Darian-Smith and Gilbert, 1994; 1995). Furthermore, the discovery of axonal sprouting of long-range horizontal connections in LPZ after a year following the lesions, indicates that these connections are likely to be involved in functional reorganization (Darian-Smith and Gilbert, 1994). However, since the experimental design was based on postmortem analysis, the dynamics of how the process of sprouting evolves is unknown. Whereas the long term remapping can be logically attributed to the increased density of horizontal connections, it is not known whether the rapid RF shifts that occur immediately after the lesion (Gilbert and Wiesel, 1992) are

accompanied by corresponding structural changes. An alternative substrate for the rapid RF shifts could be alterations in synaptic weight of existing connections, with the more extensive remapping that occurs over longer time periods being mediated by axonal sprouting. However, there is precedence for rapid structural changes. Developmental studies show that sprouting can be quite rapid (on the order of hours to days) in *Xenopus* tadpoles (Witte et al., 1996), cortical axons in the mouse (Portera-Cailliau et al., 2005) and horizontal connections in kittens (Antonini and Stryker, 1993b). Is it possible that sprouting in the adult brain recapitulates the progression of processes that occur during axonal development? During development in the mammalian brain, there is an initial exuberance of axonal connections followed by a phase of activity-dependent pruning (Hubel et al., 1977; Stanfield et al., 1982; Callaway and Katz, 1990; Antonini and Stryker, 1993a; Chen and Regehr, 2000).

An *in vivo* longitudinal study, where one images the same axons week after week, would allow us to determine the dynamic nature of the modifications immediately after the retinal lesions as well as subtle changes not detectable in a statistical study comparing structures among different

animals. During development, axon elaboration involves the growth of axonal tips and the formation of new processes by branching. During the refinement period, two different mechanisms of pruning are involved, retraction and degeneration. It seems that the process by which axon segments are eliminated is determined by the degree of modification needed: small branches are eliminated by retraction of the axonal tip whereas degeneration takes place to remove whole axonal segments (Luo and O'leary, 2005; Low and Cheng, 2006). One interesting question that our *in vivo* approach could answer is whether the process of sprouting in the adult resembles the dynamic observed during development. To perform these studies, however, we faced two complications: the ability to permanently label and to image neurons *in vivo* in non-human primates.

1.5 VIRAL VECTORS AS A TOOL TO LABEL NEURONS *IN VIVO*

To perform the experiments in non-human primates we have to be able to label the neurons *in vivo*. The impracticality of having transgenic non-human primates presents an inconvenience in labeling specific neuronal circuits. Fortunately, viral vector-mediated gene transfer could overcome

this problem, allowing us to manipulate the transcriptome of a cellular population. Historically, there has been an inability to infect non-dividing cells. However, the development of several recombinant viral vectors that can infect neurons successfully, such as adenovirus, adeno-associated virus (AAV), herpes simplex virus and lentivirus, has provided us with new tools to study the adult central nervous system. AAV vectors are very useful since they are efficiently taken up by neurons and transgenes tend to express preferentially in neurons relative to glia (Kaplitt et al., 1994; Bartlett et al., 1998; Ehrengruber et al., 2001; Stettler et al., 2006). Another advantage of this particular virus is that the expression is sustained for a long period of time.

1.6 TWO PHOTON MICROSCOPY

Light microscopy has the ability to perform observations at relatively high spatial resolutions. However, the ability to perform three-dimensional reconstruction inside living tissues is hampered by light scattering, causing degradation of resolution and contrast. Imaging deeper into the tissue is progressively more difficult until it becomes impossible. Confocal

microscopy was conceived to solve these problems (Minski, 1961). By focusing the illuminating light into a limited focal plane and collecting only those photons coming from the focused region (a detector pinhole rejects those photons from out-of-focus light), the spurious scattered photons are reduced allowing a better resolution. The main disadvantage of this approach is that not only the focal plane is excited by the illuminating light but also regions above and beyond, while the only information being collected is from the focal plane. This unnecessary excitation can cause the photodestruction of fluophore that was not yet imaged (photobleaching) and damage of the biological tissue by the light (photodamage). Performing *in vivo* imaging using a confocal microscope is then limited.

Two-photon microscopy can solve all of these problems by using multiphoton optical absorption (Denk et al., 1990). Instead of using a single photon with enough energy to excite a fluophore, it is based on the possibility of absorbing more than one photon with suboptimal energy during a single quantum event (Goeppert-Mayer, 1931). By using femtosecond Ti:sapphire laser pulses, only in the vicinity of the focal volume, where the intensity of the light is high, a fluorophore can receive

enough energy to be excited. Outside this volume, the illuminating light has insufficient energy, eliminating photons from the specimen coming from out-of-focus regions. Therefore, since a pinhole is not necessary all the photons from the sample constitute useful signal. Since longer excitation wavelengths are being used (around twice of what would be used by single-photon excitation), the infrared light can penetrate deeper into the tissue.

AAV labeling of neurons coupled with two-photon microscopy allows us to uncover the extent of neuronal plasticity in the living brain. In the first part of our current study, we performed longitudinal studies to determine the structural dynamics of cortical axons and boutons without alterations in visual experience. In the second part, we further characterize the degree of plastic changes of neuronal circuits in the adult brain by investigating the functional reorganization caused by deprivation of visual input.

2 AXONS AND SYNAPTIC BOUTONS ARE HIGHLY DYNAMIC IN ADULT VISUAL CORTEX

Dan D. Stettler[1], Homare Yamahachi[1], Wu Li[1], Winfried Denk[2] & Charles D. Gilbert[1]

1 Laboratory of Neurobiology, The Rockefeller University

2 Max Planck Institute for Medical Research, Heidelberg, Germany

Neuron 49, 877 - 887 (2006)

2.1 SUMMARY

While recent studies of synaptic stability in adult cerebral cortex have focused on dendrites, how much axons change is unknown. We have used advances in axon labeling by viruses and *in vivo* two-photon microscopy to investigate axon branching and bouton dynamics in primary visual cortex (V1) of adult Macaque monkeys. A nonreplicative adeno-associated virus bearing the gene for enhanced green fluorescent protein (AAV.EGFP) provided persistent labeling of axons, and a custom-designed two-photon microscope enabled repeated imaging of the intact brain over several weeks.

We found that large-scale branching patterns were stable but that a subset of small branches associated with terminaux boutons, as well as a subset of en passant boutons, appeared and disappeared every week. Bouton losses and gains were both ~7 % of the total population per week, with no net change in the overall density. These results suggest ongoing processes of synaptogenesis and elimination in adult V1.

2.2 INTRODUCTION

Synaptic stability critically affects the function of brain circuits and could be necessary to maintain the integrity of neuronal functional properties. At the same time, alterations in cortical responses observed during perceptual learning or disruptions of sensory input might result from changes in connectivity that requires synaptic pliability. Physiological plasticity could be mediated through synaptic changes at multiple spatial and temporal scales. Among other possibilities, synapses might be formed or eliminated through rearrangements of morphological structures such as dendritic spines and axon boutons. These rearrangements could occur either by small-scale alterations along stable neuronal processes or as the result of

larger-scale changes in those processes. Studies in the cortex of adult mice suggest that spine morphology is mutable even under conditions where no training or disruption of input has occurred, though the degree of changeability is still debated (Grutzendler et al., 2002; Trachtenberg et al., 2002; Holtmaat et al., 2005 and Zuo et al., 2005; at the end of the critical period: Majewska and Sur, 2003). It is unknown, however, whether axons and their boutons undergo morphological alterations in the normal adult cortex.

Recent advances have been made in the *in vivo* imaging of axons during development in mouse cortex (Portera-Cailliau et al., 2005) and in the midbrain of *Xenopus* (Cohen-Cory and Fraser, 1995; Alsina et al., 2001; Foa et al., 2001; Ruthazer et al., 2003; Hu et al., 2005), goldfish (during regeneration: Johnson et al., 1999), and zebrafish (Schmidt et al., 2000; Schmidt, 2004; Hua et al., 2005), as well as during development or adult plasticity in the spinal and peripheral circuitry of mouse, *Xenopus*, and zebrafish (Colman et al., 1997; Gan and Lichtman, 1998; Jontes et al., 2000; Buffelli et al., 2003; Kasthuri and Lichtman, 2003; Walsh and Lichtman, 2003; Bhatt et al., 2004; Bishop et al., 2004; Flanagan-Steet et al., 2005;

Javaherian and Cline, 2005; Kerschensteiner et al., 2005; Liu and Halloran, 2005; Schaefer et al., 2005). In the mouse, studies of axon development and dendritic stability have been carried out in animals that have been transgenically manipulated to express label in subpopulations of cells. We wished to study alterations in cortical circuitry in primates (Macaque monkeys), where transgenic approaches are impractical yet for which a large body of work has established conditions for plasticity of receptive field properties. In Macaque V1, for example, neuronal response properties can change as a result of training or disruption of input (Gilbert et al., 1990; Kaas et al., 1990; Chino et al., 1991; Heinen and Skavenski, 1991; Gilbert and Wiesel, 1992; Das and Gilbert, 1995; Crist et al., 2001; Schoups et al., 2001; Li et al., 2004). *In vivo* imaging of neuronal morphology in the Macaque has, however, faced the dual challenges of developing a means for long-term labeling of neurons and their processes with fluorescent probes and the need for a multi-photon microscope capable of accommodating large animals. These issues were addressed by using viral labeling of cortical neurons and developing a customized two-photon microscope (Denk et al., 1990).

Advances in the delivery of genetically encoded fluorophores have made it possible to completely label neurons and their processes in many species. A nonreplicative adenovirus (Ad) bearing the EGFP gene has been shown to provide effective labeling of adult cortical neurons without the need for histological processing (Stettler et al., 2002). While Ad.EGFP strongly and consistently labels somata, dendrites, and axons, it is of limited use for longitudinal studies because its labeling starts to decrease a couple of weeks after infection. Therefore, nonreplicative AAV.EGFP was tested as an alternative based upon its ability to drive long-term expression in adult neurons (Chamberlin et al., 1998; Bennett et al., 1999).

Two-photon imaging of neurons in the intact brain, originally demonstrated in rodents (Svoboda et al., 1997), is based on the confinement of excitation to a narrow focal plane and excitation at infrared wavelengths, which allow light penetration deep within cortical tissue (Denk and Svoboda, 1997). One limitation of two-photon microscopy for larger animals is the need to move the imaged sample relative to the microscope's objective. To solve this problem, a microscope was custom-fitted with a second scanning head and a moveable objective to allow scanning over a

large area while keeping the animal stationary. This arrangement, combined with a specially designed chamber that provides a window over V1, permitted repeated imaging of the same positions in Macaque V1. Using these techniques, we studied changes in the axons of adult Macaque visual cortical neurons that occur without the imposition of a systematic change in visual experience either through lesioning or training.

2.3 RESULTS

2.3.1 PERSISTENT LABELING AND *IN VIVO* IMAGING

To test the labeling strength and persistence of the AAV.EGFP technique, high-titer injections were made into V1 of adult mice. Following the injections, EGFP labeling developed in neurons and glia within 3–4 weeks. Single time point *in vivo* two-photon microscopy of labeled cells and axons in mouse V1 established that labeling was visible in the intact brain (Fig. 2.1A). The extent of cortical territory containing labeled cells depended on the injected volume, and bodies of labeled cells could be readily identified. In two cases, injected mice were examined after long survival periods, without interceding imaging sessions, to assess the

persistence of the label. We found that cell bodies (Fig. 2.1B) and processes, including axons (Fig. 2.1C) remained well-labeled and appeared normal 1 year after viral injection.

AAV.EGFP injections in V1 of adult Macaques produced similar labeling (Fig. 2.1D and 2.1F). In intact Macaque V1, EGFP-labeled somata and processes were discernible at high resolution to depths as far as 500 μm below the surface. Because superficial blood vessels cast shadows over imaged regions, somata and processes stretching over hundreds of micrometers were sporadically interrupted by linear dim regions. The virus produced strong (but not exclusive) labeling of pyramidal cells (Fig. 2.1E) with well-filled spiny dendrites (Fig. 2.1F) and axons (Fig. 2.2). As in the mouse, strong labeling was maintained over long postinjection periods in the Macaque. The longest postinjection period tested in a Macaque was 5 months.

Figure 2.1. Strong and Persistent AAV.EGFP-Mediated Labeling of Macaque and Mouse V1 Neurons Imaged *In Vivo* with Two-Photon Microscopy

(A) Mouse V1 neurons labeled with AAV.EGFP and imaged *in vivo*. This montage was assembled from projections of Z stacks acquired through a depth of 200 μm. Imaging was performed 4 weeks after injection. These and subsequent images of EGFP-labeled neurons have been filtered with a 2.0 pixel Gaussian filter to remove noise. These projections and others in this figure were calculated by maximum intensity.

(B) Injection site in mouse V1 imaged postmortem in a 50 μm section cut tangential to the cortical surface 1 year after injection of AAV.EGFP. The cell bodies remain strongly labeled and have normal morphology.

(C) AAV.EGFP-labeled mouse V1 axons 1 year after injection. The strongly labeled axons appear normal, with clearly identifiable boutons separated by narrower interbouton shafts.

(D) Macaque V1 cells labeled with AAV.EGFP and imaged *in vivo*. Strong labeling of cell bodies and processes is evident in this montage of projections from Z stacks acquired through a depth of 300 μm in the intact cortex. Most labeled cell bodies lay within the densely labeled injection site at top, though some cell bodies also appear >100 μm away. The projections include data from every third z section.

(E) Cell indicated by the arrowhead in (D) at higher magnification. Note the spiny dendrites characteristic of excitatory neurons in cortex.

(F) Close-up of a spiny dendrite.

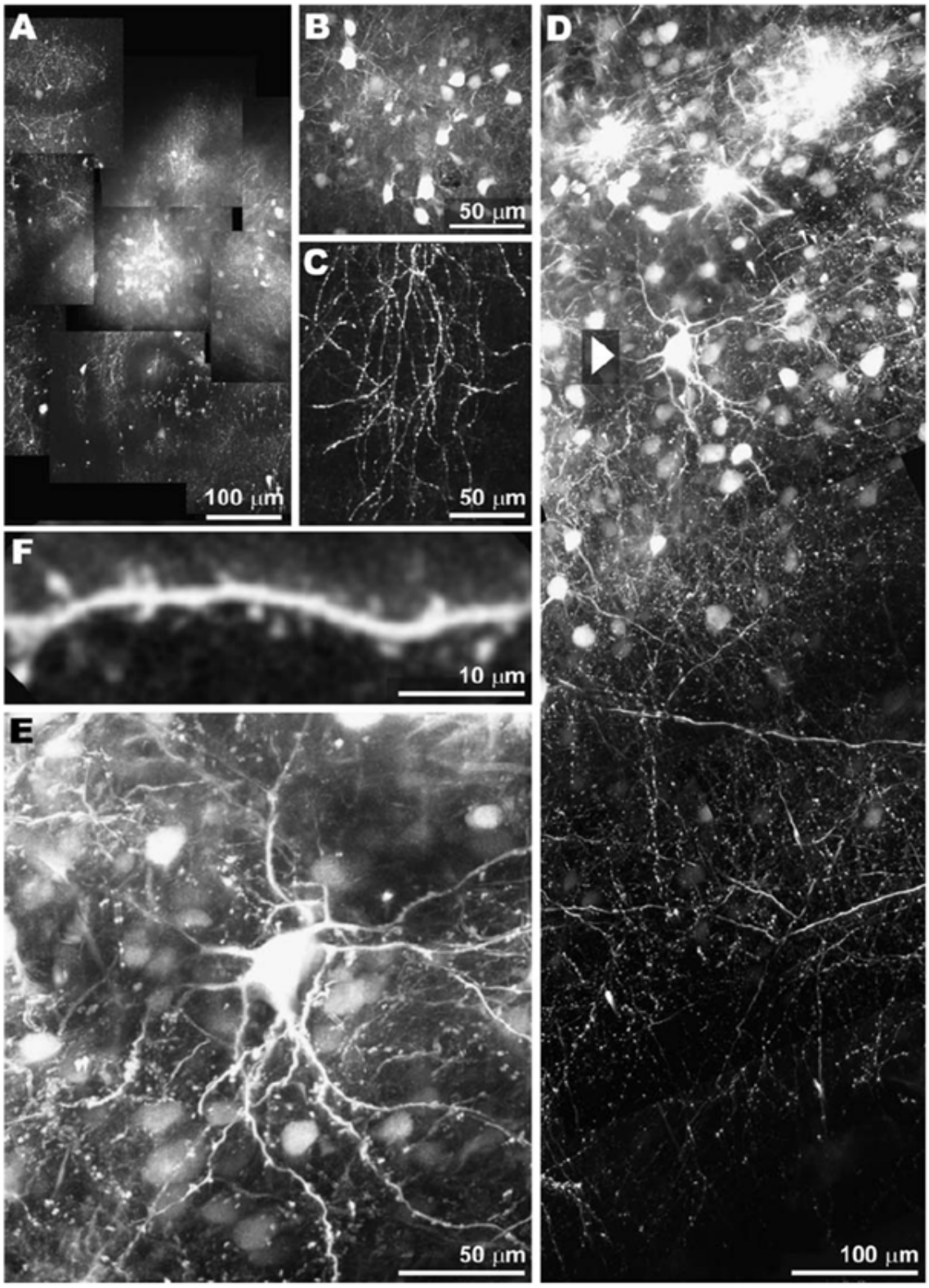
A
100 μm
B
50 μm
C
50 μm
D
100 μm
F
10 μm
E
50 μm

Figure 2.2. Similar Interbouton Distances of Axons Imaged *In Vivo* to Those Imaged in Postmortem Slices

(A and B) Axon arbors from Macaque V1 labeled with AAV.EGFP and imaged *in vivo*. The thicker portion of each axon in the lower left has little modulation of width but gives rise to multiple branches with distinguishable boutons. For much of these arbors, both en passant and terminaux boutons are unambiguously identifiable.

(C) For some axon segments, terminaux boutons (indicated with blue arrowheads) were also observed on the tips of small side branches.

(D) Distributions of *in vivo* bouton lengths (parallel to axon collateral) and widths (n = 291).

(E) Distributions of interbouton distances for axon segments imaged *in vivo* (red) and in postmortem slices (gray; n = 297 *in vivo* and 111 in slices).

(F–H) Sample images of axon segments with bouton positions schematically represented in (I).

(I) Schematic representations of bouton positions along axon segments are ordered from the highest average interbouton distance to the lowest, with the values (in micrometers) indicated at the left of each segment. Scale bar applies to all images and (I).

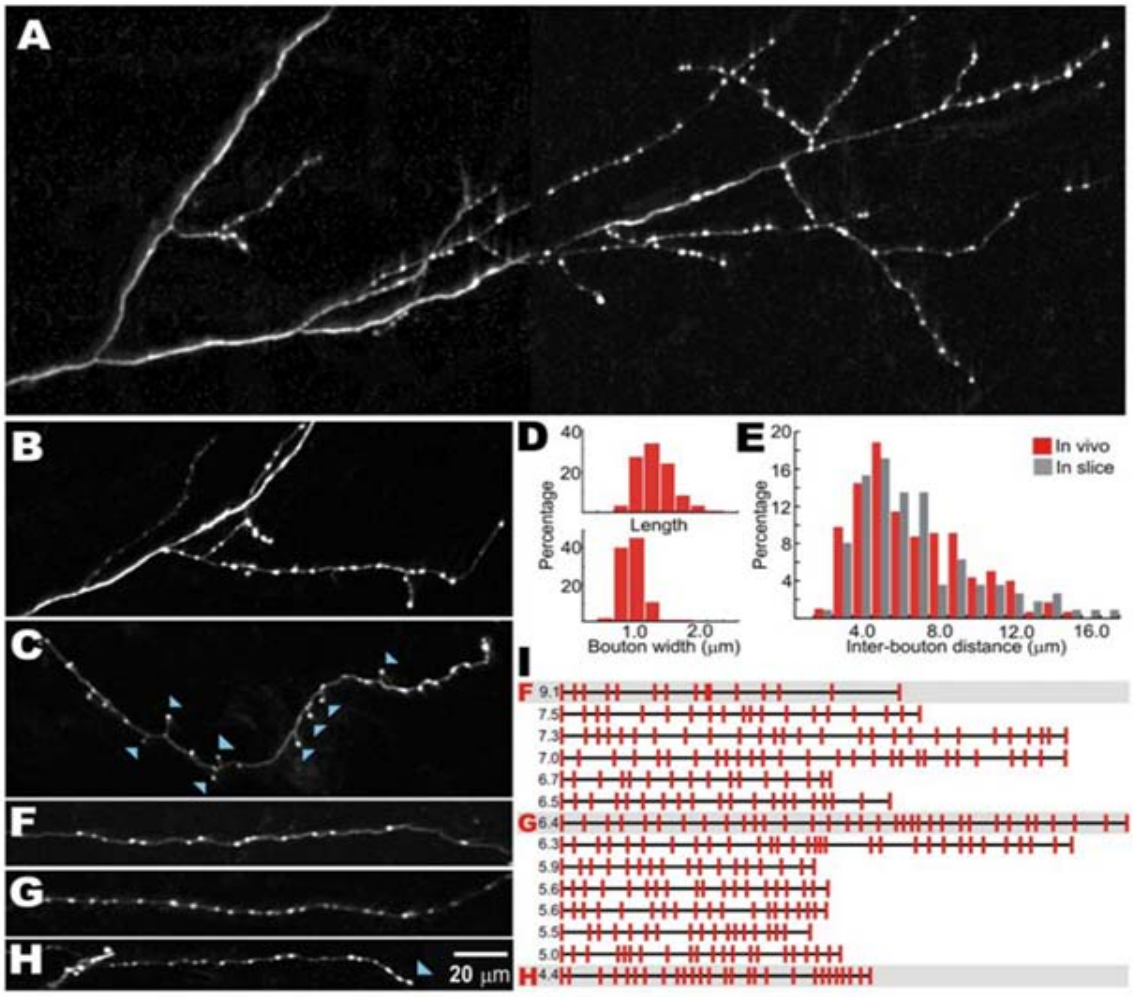
A
B
C
F
G
H
20 μm
D
Percentage
Length
Bouton width (μm)
E
In vivo
In slice
Percentage
Inter-bouton distance (μm)
I
F
G
H

2.3.2 BOUTON NUMBERS *IN VIVO* AND POSTMORTEM

Axons projecting from superficial (layers 1–3) neurons in Macaque V1 were labeled using AAV.EGFP and imaged *in vivo* through the superficial layers using two-photon microscopy (Fig. 2.2). These axons were also imaged in the superficial layers. Boutons were identified as swellings along thinner axon shafts and measured 0.5 – 2.2 μm in length (mean = 1.2 ± 0.02 μm) and 0.5 – 1.5 μm in width (mean = 0.8 ± 0.01 μm; Fig. 2.2D). Boutons were typically visible in two to three adjacent sections in acquired Z stacks.

Some axon segments lacked boutons over most of their length but gave rise to distal branches with well-defined boutons (Fig. 2.2A and 2.2B). Both terminaux and en passant boutons were observed, the former indicating the ends of axon branches (Fig. 2.2B and 2.2C). Boutons terminating larger branches often were bigger than others. Interbouton distances on superficial layer Macaque V1 axons, imaged *in vivo* or in postmortem slices (Fig. 2.2E), were on the average 6.3 ± 0.19 μm *in vivo* and 6.4 ± 0.38 μm postmortem in

sections of perfused tissue. Individual axon segments exhibited a range of average interbouton distances (Fig. 2.2F-2.2I).

2.3.3 COMPARISON OF AXON SEGMENTS AT MULTIPLE TIME POINTS

Locations in V1 containing axons were imaged at 1 week intervals. Imaging sites were matched using the blood vessel pattern by taking low-magnification reflected light pictures of the craniotomies and comparing them with montages of two-photon images obtained from the cortical surface during the first imaging session (Fig. 2.3A). Imaged regions were between 1.5 and 3 mm from the AAV.EGFP injection sites and therefore contained labeled axons but not dendrites. These distances were also beyond the reach of dense local connections of excitatory and inhibitory cells. Moreover, while excitatory cells in deeper layers have horizontal connections that extend long distances in layers containing their somata, their projections to the superficial layers tend to have a more restricted lateral extent (Gilbert and Wiesel, 1979; Blasdel et al., 1985). Therefore, distance from the injection site, combined with distributions of boutonal

characteristics consistent with a homogeneous population (Fig. 2.2), indicate that the labeled axons were primarily the collaterals of long-range horizontal projections of superficial pyramidal cells.

Z stacks acquired through the superficial layers of V1 at 1 week intervals contained axon segments that could be identified and compared across time points (Fig. 2.3B; imaging site indicated in Fig. 2.3A). Regions containing many collaterals were separated by areas with fewer axons. Such modulation of density was expected due to the patchy character of the horizontal connections in Macaque V1 (Gilbert and Wiesel, 1979; Rockland and Lund, 1982; Gilbert and Wiesel, 1983).

Figure 2.3. Axon Branching Assessed at Multiple Time Points

(A) Low-magnification reflected light image (left) of the surface vasculature over an exposed portion of V1 (position indicated in inset). The same vessel pattern can be seen in a montage (right) of superficial sections from two-photon Z stacks from that region of V1. The AAV.EGFP injection site and location of axons seen in (B) are indicated. Scale bar, 1 mm.

(B) Projection of a field of axon segments imaged over a 100 μm depth 1 week apart. Before calculating the projections by maximum intensity, portions of individual z sections without axons were set to zero intensity to reduce background fluorescence. Most axons are visible at both time points. (Right) Individual axons were matched in the two data sets and traced in the Z stacks (after processing with a 2 pixel Gaussian filter to reduce noise followed by brightness and contrast adjustment). Portions of some axons were not clearly visible during all imaging sessions due to growth of connective tissue on the surface of the cortex. Comparison of only those segments of axons that were clearly visible at multiple time points revealed no changes in the large-scale (>10 μm) branching patterns of axons. For a close-up of the axon segment in the blue box, see Fig. 2.4, and for that in the red box, see Fig. 2.6.

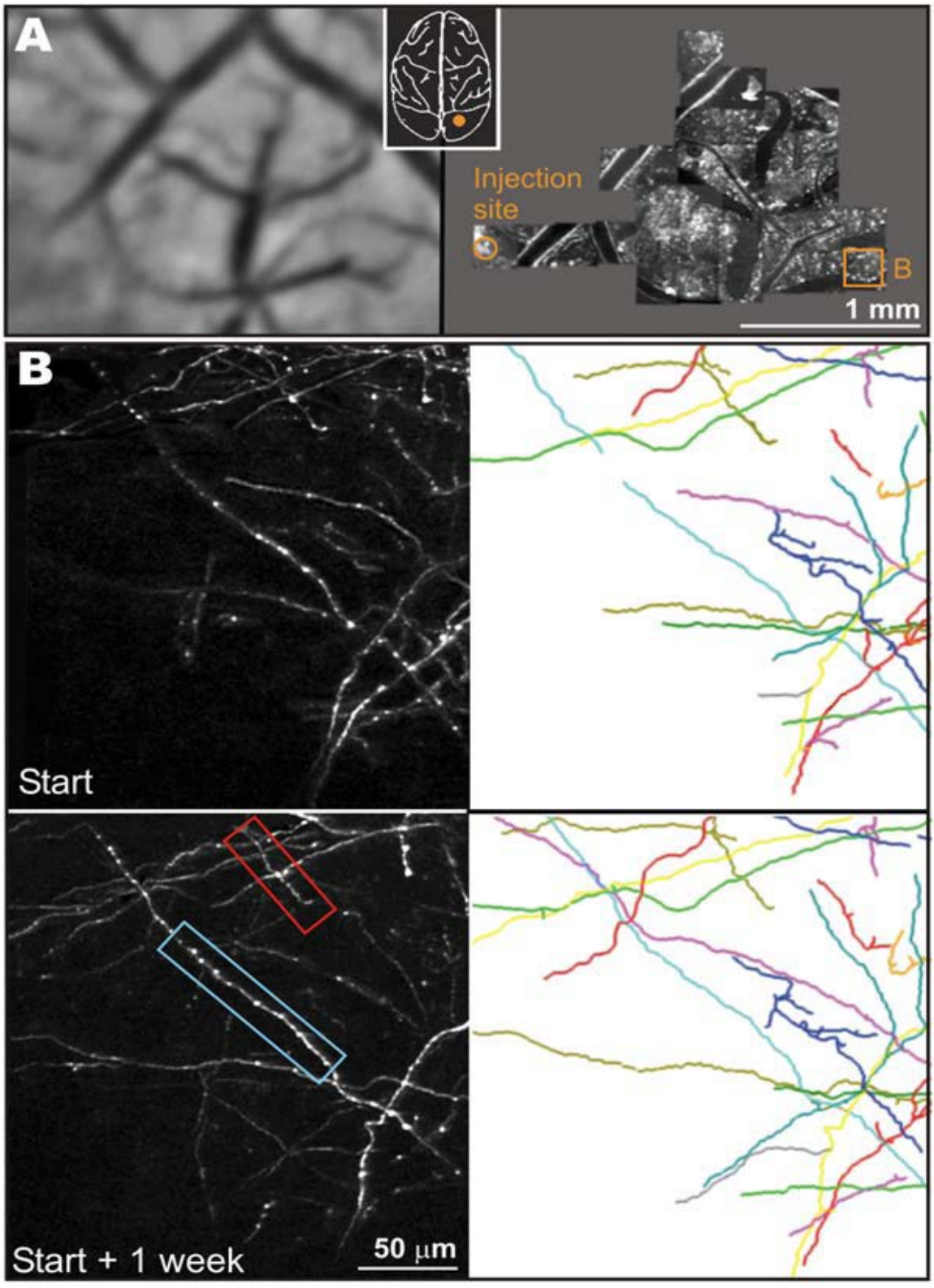
A
Injection
site
B
1 mm
B
Start
Start + 1 week
50 μm

Unlike the mouse, where dura (and even the thinned skull) are transparent enough for two-photon microscopy, the Macaque has a thick, opaque dura that must be removed before imaging. Removing the dura does not compromise the health of the cortex, which retains its blood supply and pia. However, after the dura has been removed, the surface of the cortex is subject to continuous growth of connective tissue. This tissue, while initially clear to the eye, later blocks two-photon imaging. For a few weeks after dura removal, the connective tissue can be stripped off without difficulty, but eventually it cannot be removed without damaging the cortex. Consequently, not all labeled axons were visible during every session. Reduction in axon brightness resulting from surface tissue could be distinguished from dimming or disappearance of axons themselves because it was matched by a reduction in background autofluorescence at the same depth and because, on occasions when the newly grown surface connective tissue could be successfully removed, the axons beneath became brighter. Because the presence of surface tissue is unlikely to be correlated with changes in connectivity in the underlying cortex, we chose axon segments for comparison across time points only if they appeared bright and their

branching morphology was clearly discernible during all compared imaging sessions.

The same axons were identified at multiple time points and traced to determine their length. The dynamics of gross axon morphology were examined by counting how frequently new branches formed or existing branches disappeared and, when such changes were found, by how much the axon length changed. In total, 5.87 mm of axon in 16 locations from 2 animals was compared across two time points separated by 1 week. Axon branching remained largely stable with no branches longer than 11 μm appearing or disappearing (see below).

2.3.4 EN PASSANT BOUTON DYNAMICS

A subset of those axon segments that were compared over multiple time points had a morphology that was well enough defined to allow analysis of boutons. In all, 221 en passant boutons on 19 axon segments with a total length of 1.57 mm were compared in two animals. Frequent bouton additions and eliminations along collaterals were observed (Fig. 2.4

and 2.5). These changes were independent of depth through the superficial layers. For each animal, the number of boutons added was similar to the number eliminated. The frequencies of these changes were similar between animals. In animal 1, which initially had 175 boutons on the tested segments, 11 (6.3 %) of those boutons disappeared while 11 new en passant boutons appeared during 1 week. In animal 2, the numbers were as follows: 49 initial boutons, 4 (8.2 %) appeared, 3 disappeared (6.1 %). We only counted a bouton as having disappeared if the axon shaft at that location was discernible and the pattern of nearby boutons remained unchanged.

Figure 2.4. Boutons Added and Eliminated along Existing Axon Collaterals

At top, the same axon at three time points separated by 1 week intervals. The images are "cut-and-paste" projections in which the clearest representation of the axon at a given position was cut out of a single z section and compiled with representations of other positions from other z sections. This method reduces the distortions of local contrast produced by noise and autofluorescence in maximum intensity projections, but neither method conveys the full amount of information present in the Z stacks, which were used for analyses of bouton appearances and disappearances. The image sets below are sample individual optical sections selected from the Z stacks containing the axon. The right portion of this axon was bright at all three time points, but some boutons on the left portion could not be compared for the first time point due to dimness at that location during that imaging session. Red triangles mark boutons that did not change between time points. Yellow and green triangles mark disappeared and appeared boutons, respectively. The orange triangle marks a site where a bouton was present only during the second imaging session. Pink triangles mark sites that, during the first time point, could not be compared due to the dimness of the axon.

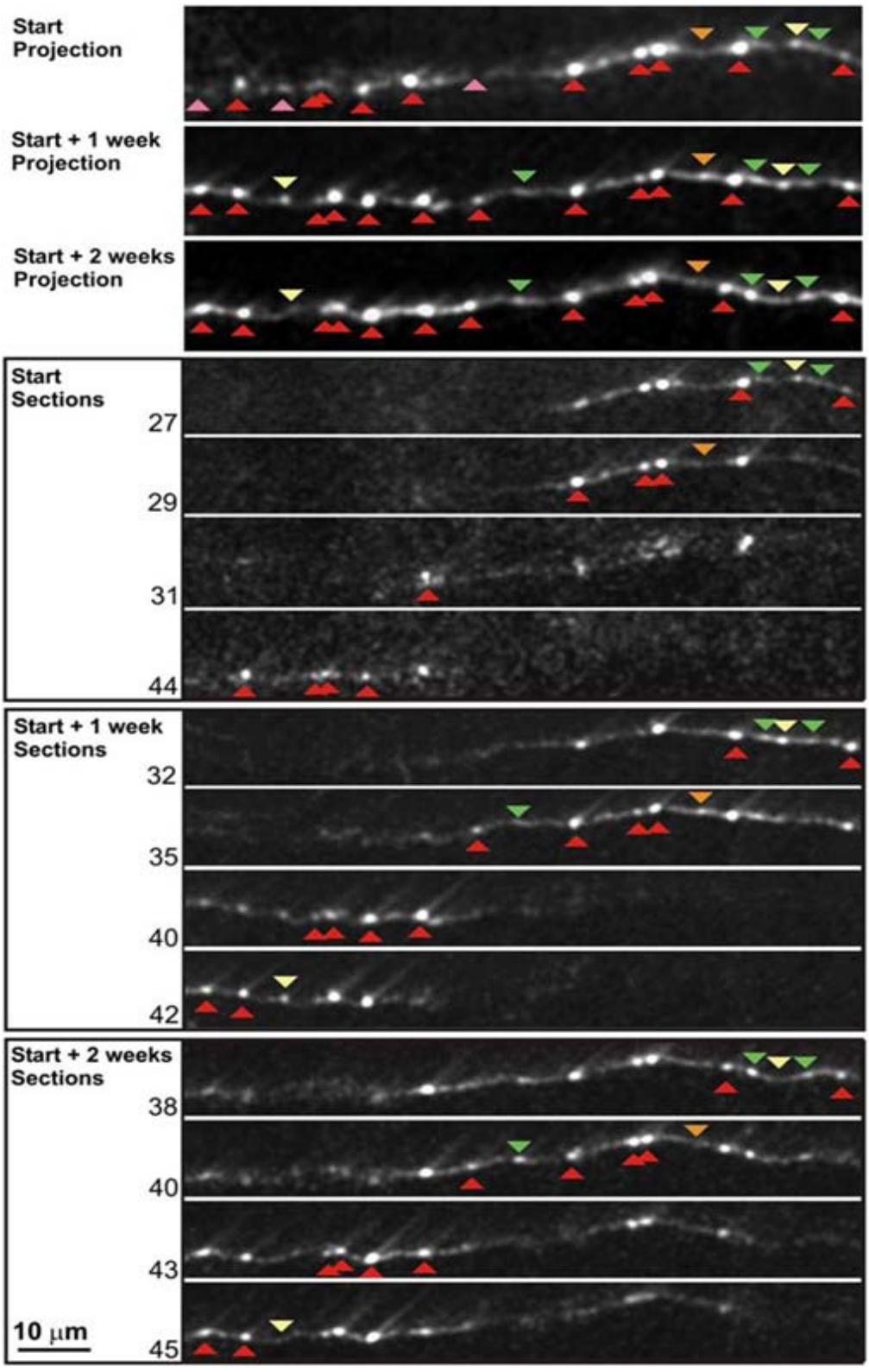
Start
Projection
Start + 1 week
Projection
Start + 2 weeks
Projection
Start
Sections
27
29
31
44
Start + 1 week
Sections
32
35
40
42
Start + 2 weeks
Sections
38
40
43
45
10 μm

Figure 2.5. Additional Examples of En Passant Boutonal Dynamics

(A) An axon segment in which one new bouton was added and two boutons were eliminated over 1 week. (Color conventions as for Figure 2.4) The top two panels depict cut-and-paste projections of the axon at two time points separated by 2 weeks. In the lower two panels, the projection of the "Start" time point has been stretched to aid the visual inspection of matching boutons.

(B–F) High-resolution views of three added (B–D) and two eliminated (E and F) boutons. Scale bar in (F) is correct for (B)–(F).

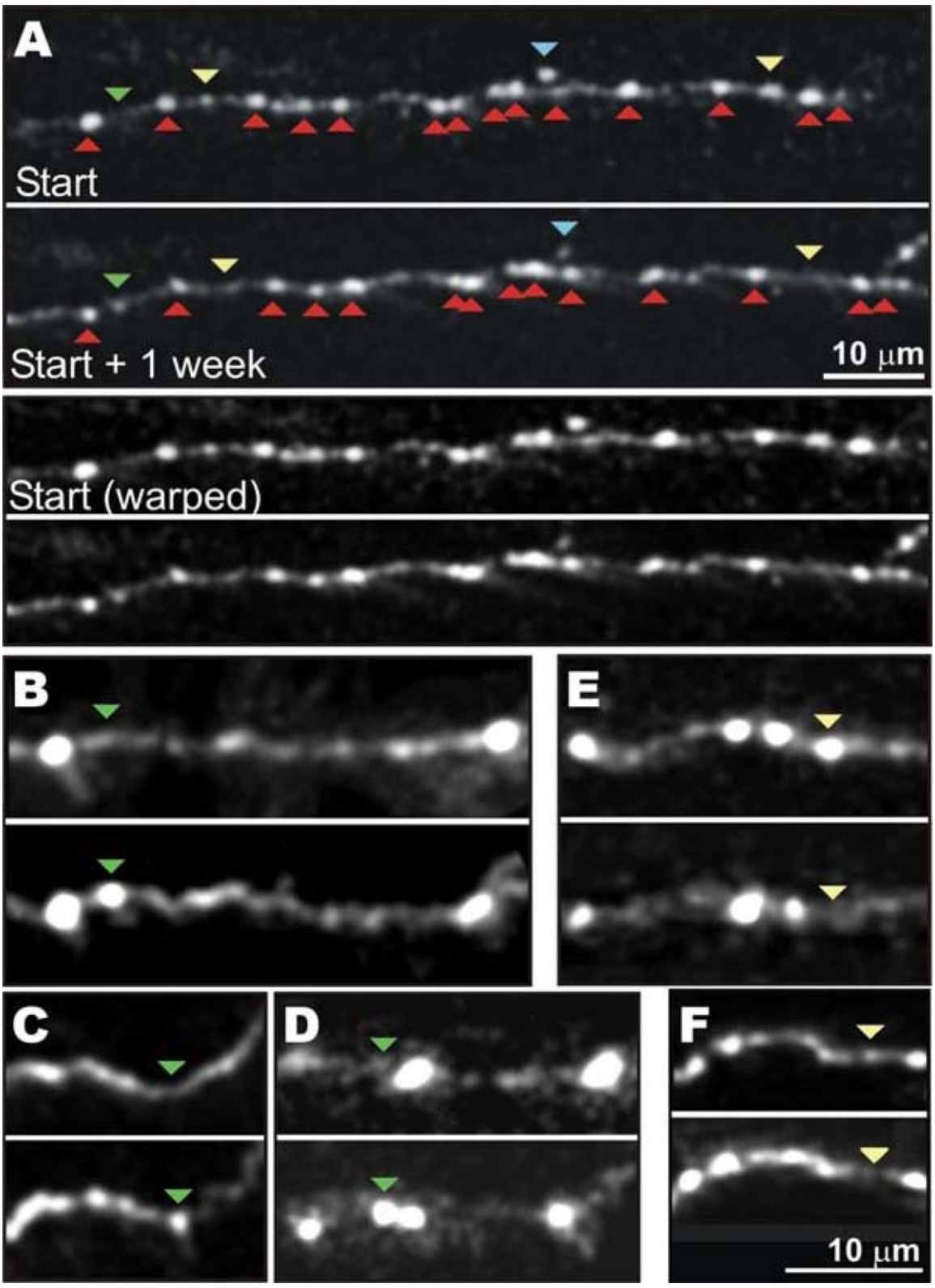
A
Start
Start + 1 week
10 μm
Start (warped)
B
E
C
D
F
10 μm

Some boutons were examined over a longer interval. Changes over a 2 week period (initial number = 50) included seven additions (14 %) and six eliminations (12 %) were about twice those observed over 1 week. Forty boutons were examined at three time points (start, start + 1 week, and start + 2 weeks). In this group, one bouton was added during the first week and eliminated during the second week (Fig. 2.4).

2.3.5 TERMINAUX BOUTON DYNAMICS

Large-scale changes in axon branching that involved additions or subtractions of axon collaterals longer than 11 μm were not observed. However, small side branches along axon shafts, nearly always bearing terminaux boutons, did appear (Fig. 2.6A and 2.6B) and disappear (Fig. 2.6A-2.6C). The set of axon segments examined for en passant bouton changes (total length 1.57 mm) possessed 22 side branches with terminaux boutons during the first imaging session. During a 1 week period, three side branches were subtracted and three new side branches having terminaux boutons were added. The entire set of axon segments examined for large-scale branching patterns (5.87 mm total) initially possessed 55 side branch

terminaux boutons, with an average length of 4.2 ± 0.39 μm. During a 1 week interval, nine of these side branches were lost (with average length 3.1 ± 0.4 μm) and six new side branches bearing boutons were generated (4.3 ± 01.0 μm). These alterations were always less than 11 μm over a 1 week interval. The higher level of turnover exhibited by terminaux versus en passant boutons is significant ($\chi^2 = 5.14$; df = 1; $p < 0.05$; losses and gains were pooled).

Figure 2.6. Extension and Contraction of Bouton-Bearing Side Branches
(A) Extension of a small side branch and contraction of another one, both with terminaux boutons, over 1 week.
(B) Axon segment with multiple side branch changes over 1 week.
(C) Contraction of a small side branch with a terminaux bouton.

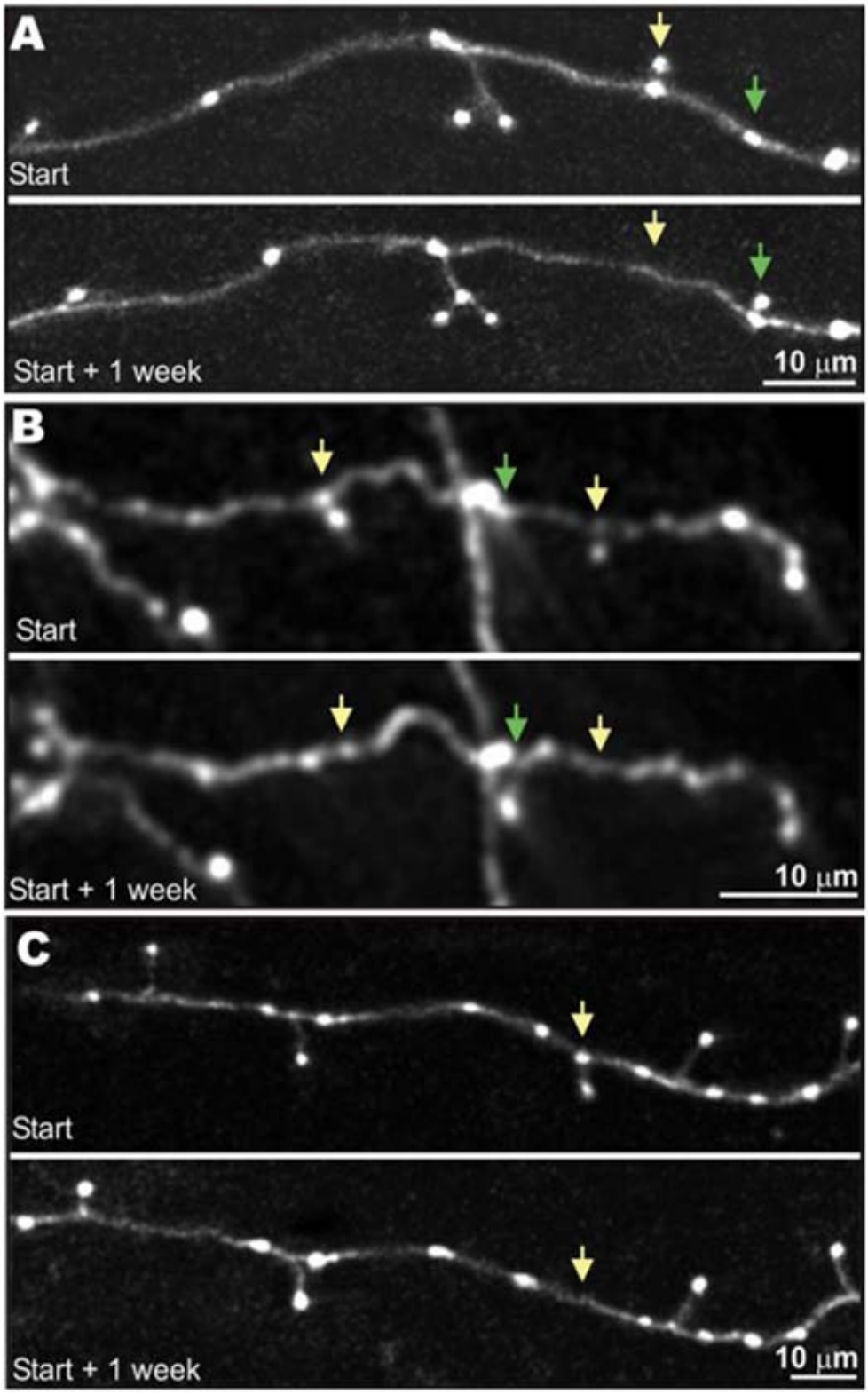
A
Start
Start + 1 week
10 μm
B
Start
Start + 1 week
10 μm
C
Start
Start + 1 week
10 μm

Most often, the changes in side branches involved the elimination or addition of the whole branch, including its bouton. In one case, however, an expansion from the tip of an existing side branch was observed that maintained the original bouton and added another, now terminaux, bouton. Also in one case, a terminaux bouton disappeared from a small branch containing a second, more proximal bouton that then became the terminaux bouton.

During one imaging session, a small branch that had appeared since the previous week's imaging session contracted over a period of 2 hr (Fig. 2.7). The branch did not have a bouton at the start of the second session, so it is unclear whether it was a terminaux bouton caught in the process of disassembling or a filopodium that had never possessed a bouton. This lone observation is nevertheless intriguing given the higher turnover observed among the population of terminaux boutons compared to that of en passant boutons. The total rate of bouton turnover over a 1 week interval, including terminaux and en passant boutons, was therefore about 7 %.

Figure 2.7. Fast Side Branch Dynamics

An axon segment during the initial imaging session (top) and then at multiple time points during the second session 1 week later. All images are projections. Note the small side branch (11 μm long) present at the beginning of the second session. This side branch contracted during the following 2 hr and did not reappear during the rest of the session. Most other features of the segment, including two terminaux boutons (blue arrowheads), remained unchanged.

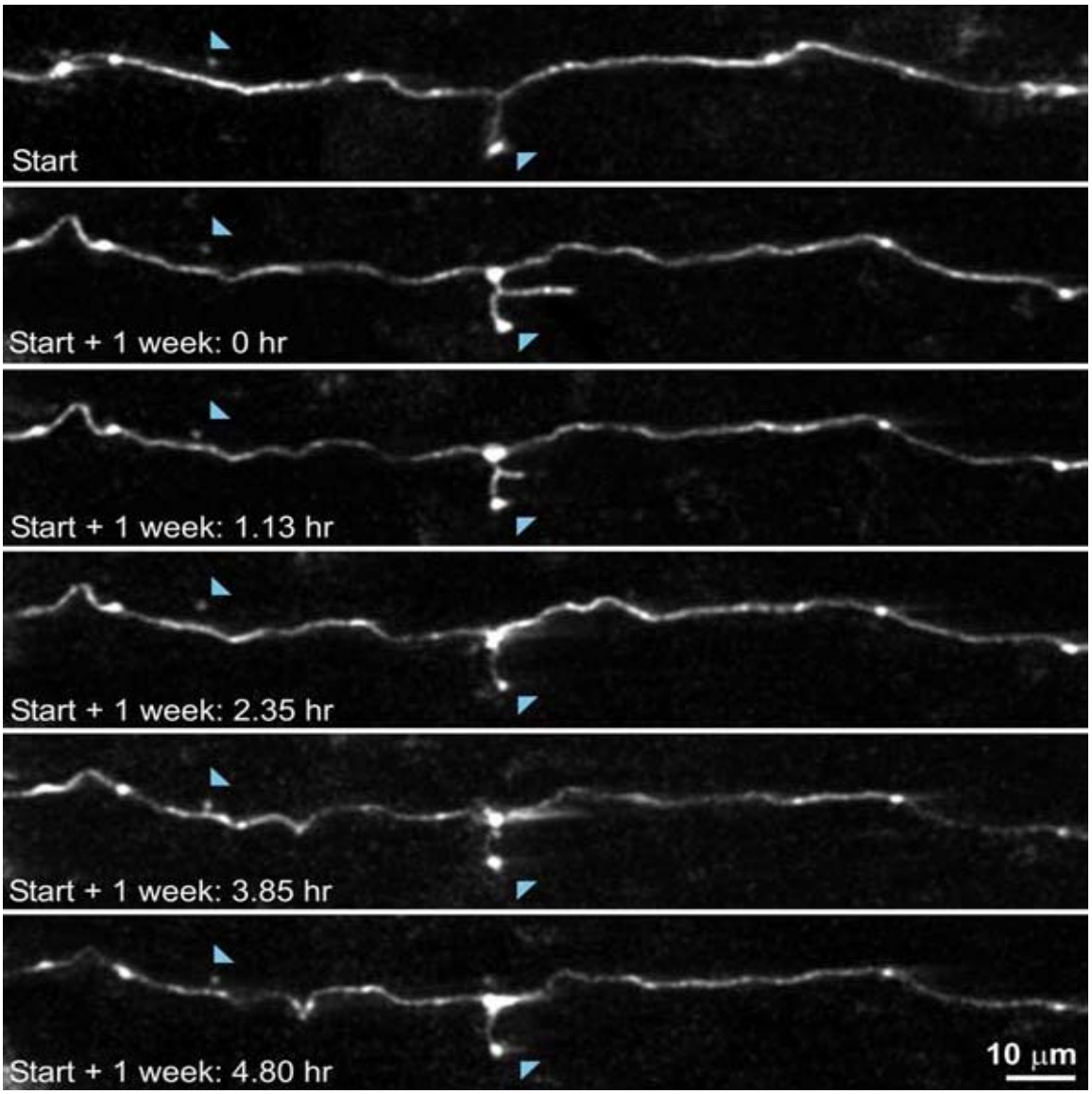
Start
Start + 1 week: 0 hr
Start + 1 week: 1.13 hr
Start + 1 week: 2.35 hr
Start + 1 week: 3.85 hr
Start + 1 week: 4.80 hr
10 μm

2.4 DISCUSSION

The combination of persistent axon labeling, using AAV.EGFP, with *in vivo* two-photon imaging permits the comparison of selected axon segments longitudinally in time. We found that the morphology of long-range horizontal connections in intact V1 of adult Macaques was mutable on a short length scale (less than ~10 μm) on the time scale of 1 week. The overall rate of bouton turnover was about 7 % per week, but the total number of boutons remained largely unchanged. A similar stability of large-scale axon branching patterns but pronounced mutability of terminaux and en passant boutons has recently been found for intracortical axons in barrel cortex of the mouse (De Paola et al., 2006). These changes in axon morphology suggest that substantial genesis and elimination of synaptic connections occur in the adult cortex.

2.4.1 BOUTON DESIGNATION AND PREDICTION OF EFFECTIVE SYNAPSES

The general agreement between the average interbouton distance seen *in vivo*, 6.3 μm, with that observed in postmortem cortical slices here and in other reports (Amir et al., 1993; mouse: Braitenberg, 1998; cat: Anderson et al., 2002) indicates that our imaging technique had sufficient resolution to assess a representative population of boutons and that our criteria for identifying boutons matched those of earlier studies.

The appearance and disappearance of boutons observed in this study are very likely to reflect the formation and elimination of synapses. Neuronal morphological parameters have increasingly been found to relate to the existence and strength of synapses. Numerous studies of cortical axons have established that, when boutons are identified under light microscopy and subsequently examined with electron microscopy, nearly every bouton has at least one synapse, and synapses on axonal shafts between boutons are extremely rare (Somogyi, 1978; Peters and Proskauer, 1980; Winfield et al., 1981; Somogyi et al., 1982; Schuz and Munster, 1985;

Kisvarday et al., 1986; Friedlander et al., 1991; Mcguire et al., 1991; Peters et al., 1991; Anderson et al., 1998; Braitenberg, 1998; Kincaid et al., 1998; Schikorski and Stevens, 1999; Anderson and Martin, 2001; Lubke et al., 2003; Silver et al., 2003; Anderson and Martin, 2005). Due to the distance from the injection sites at which imaging was performed for this study, the imaged axons were predominantly the intrinsic long-range horizontal connections of superficial pyramidal cells (discussed below). For the intrinsic axons of pyramidal cells, all the boutons identified by light microscopy have been found by electron microscopy to form at least one synapse (Somogyi, 1978; Schuz and Munster, 1985; Mcguire et al., 1991). Moreover, the lost and gained boutons observed in this study exhibited the same distribution of sizes as the static boutons (e.g., Fig. 2.4 and 2.5). Accumulating evidence indicates that bouton size is positively related to active zone and postsynaptic density size (Pierce and Lewin, 1994; Harris and Sultan, 1995; Schikorski and Stevens, 1997; 1999). Therefore, the appearance and disappearance of boutons observed *in vivo* with two-photon imaging is likely to provide a reliable measure for cortical plasticity.

2.4.2 BOUTON DYNAMICS IN ADULT CORTEX

Depending on whether the population of boutons is homogeneous or not, the amount of bouton turnover (7 % per week) has different implications for the stability of the synaptic connection network. If all boutons have the same replacement probability per unit time, synaptic connectivity would become largely remodeled after about 14 weeks. Alternatively, there may be a subpopulation of connections that are highly dynamic, with the rest remaining stable. The doubling of the total turnover observed with a doubling of the interval from 1 to 2 weeks is consistent with a uniform probability. However, so far only a limited number of boutons have been imaged at longer periods and more than two time points. Additional observations over longer periods and multiple time points will be necessary to resolve this issue conclusively.

For the current study, no systematic learning regimen or input disruption was used. The bouton turnover observed might nevertheless represent specific changes that were dependent on the animals' experience over the course of the experiment. An alternative possibility is that cortical

circuitry turns over independent of experience, with bouton losses and gains occurring as independent stochastic processes. In either case, the correspondence between rates of bouton addition and elimination suggests regulation of total bouton number in cortical circuits. Addition and subtraction rates for presynaptic terminals in hippocampal slices have also recently been found to be equal (De Paola et al., 2003).

Besides addition and elimination of boutons along existing axon collaterals, a subset of axons showed the extension and contraction of small side branches ending in terminaux boutons. The dynamic rearrangement of such branches, which could occur within hours (Fig. 2.7), expands the spatial range within which axons can choose their targets (Chklovskii et al., 2004). Similarly, fast changes in small-scale axon morphology have been observed in the intact mouse cortex (Dittgen et al., 2004).

The adult axon dynamics described here complement findings for dendrites in mouse cortex *in vivo* (Hering and Sheng, 2001; Grutzendler et al., 2002; Trachtenberg et al., 2002; Majewska and Sur, 2003; Chklovskii et al., 2004; Yuste and Bonhoeffer, 2004; Holtmaat et al., 2005; Zuo et al.,

2005), which show that the branching of cortical pyramidal cell dendrites remains stable in the adult. Similar stability, characterized by only low rates of small expansions and contractions under ordinary circumstances, is seen in the dendritic branching of mitral and tufted cells of the olfactory bulb (Mizrahi and Katz, 2003). In contrast to this branching stability, spine formation and elimination have been seen in cortical dendrites. Spines apparently fall into at least two stability categories: those that persist for months and those that change over the course of days and weeks, with the distribution between these categories being disputed (Grutzendler et al., 2002; Trachtenberg et al., 2002; Holtmaat et al., 2005; Zuo et al., 2005). The rate of spine turnover in the somatosensory cortex can be altered by whisker trimming (Trachtenberg et al., 2002).

While the vast majority, if not all, of presynaptic sites in cortex involve boutons, spines are located only on the dendrites of the 80 % of cortical neurons that are excitatory. Moreover, excitatory neurons receive synaptic input onto their dendritic shafts in addition to their spines (Mcguire et al., 1991). Therefore, we cannot be sure whether or not an added or subtracted bouton corresponded to a synapse onto a spine. Regardless of the

exact relationship between changing dendritic spines and boutons, the dynamic nature of axons in adult cortex demonstrated here argues against the notion that changes in connectivity are mediated only by postsynaptic structures, such as spines, choosing among static presynaptic partners.

Earlier studies in other systems employing *in vivo* imaging and less direct techniques demonstrate that axon stability is highly dependent upon the circuit in which an axon is embedded and the history of that circuit. During development, certainly, axons are universally dynamic and exhibit not only tremendous growth but also retraction or degeneration (Cohen-Cory and Fraser, 1995; Colman et al., 1997; Gan and Lichtman, 1998; Jontes et al., 2000; Alsina et al., 2001; Buffelli et al., 2003; Kasthuri and Lichtman, 2003; Ruthazer et al., 2003; Walsh and Lichtman, 2003; Bishop et al., 2004; Hu et al., 2005; Javaherian and Cline, 2005; Portera-Cailliau et al., 2005). Extensive axon regeneration in adults is observed after injury in the peripheral nervous system (recent *in vivo* imaging in the mouse: Nguyen et al., 2002 and Pan et al., 2003) or, in nonmammalian vertebrates, in the central nervous system (e.g., Johnson et al., 1999 and Bhatt et al., 2004). In V1, both thalamocortical axons and long-range horizontal connections go

through processes of elimination and elaboration during development (Hubel et al., 1977; Callaway and Katz, 1990; Antonini and Stryker, 1993a), by which they assume the large-scale organization that they maintain throughout adulthood under ordinary circumstances. This stability of axonal branching in the adult is supported by the current study. However, postmortem studies indicate that axon branching can occur in the neocortex of adult mammals following peripheral damage (discussed in the next section: Darian-Smith and Gilbert, 1994 and Florence et al., 1998). One interesting theme that has emerged from studies both during development and in the adult is that competition plays an important role in determining axonal input to postsynaptic cells. Beyond the issue of stability of axonal branching, when one examines axons at the spatial scale of boutons as we do here (which has been relatively less well-studied), we do observe dynamics in the absence of explicit experimental intervention. Even so, it appears that some types of axons in the periphery, including motor nerve terminals innervating the neuromuscular junction (Lichtman et al., 1987; Balice-Gordon and Lichtman, 1990) and preganglionic terminals in the submandibular ganglion (Gan et al., 2003), are very stable in the adult mouse, with very few contacts being added or eliminated. The greater

boutonal turnover observed here in the long-range horizontal connections of neocortex is intriguing considering recent findings showing experience-dependent changes in adult V1 associated with perceptual learning.

2.4.3 A BASELINE MEASURE OF AXON DYNAMICS

These experiments provide a baseline measure of axon and bouton dynamics in the absence of any systematic training or disruption of input. Because it is known that learning a given perceptual task leads to changes in the response properties of V1 neurons (Crist et al., 2001; Schoups et al., 2001; Li et al., 2004), it is tempting to speculate that during learning bouton turnover in the axons involved is accelerated so as to effect functional changes that underlie the learning. This may be particularly the case for those tasks that involve lateral interactions between stimuli lying within and outside of the classical receptive field and would thus require the long-range horizontal connections (Gilbert and Wiesel, 1979; Rockland and Lund, 1982; Stettler et al., 2002) that our experimental protocol specifically targets. Because horizontal connections of a given pyramidal cell may connect with each of their target cells at only a single synapse (Mcguire et al., 1991), the

addition and elimination of a small number of horizontal connection boutons might entail significant qualitative alterations in their connectivity. This nonredundancy of horizontal connectivity is not observed in the vertical circuitry of V1, which comprises relatively focused connections between cells within individual columns.

While we did not observe changes in larger-scale axon branching patterns, such changes might be more likely to occur under circumstances where gross changes in the connectivity between loci in cortex are expected, such as during intense training or disruption of input. An example is when input to V1 is disrupted by retinal lesions, which silence feedforward activation in small cortical "scotomas" and which lead, over time, to a reorganization of the cortical topography (Gilbert et al., 1990; Kaas et al., 1990; Heinen and Skavenski, 1991; Chino et al., 1992; Gilbert and Wiesel, 1992; Das and Gilbert, 1995; Schmid et al., 1996; Calford et al., 2000; Smirnakis et al., 2005). Postmortem analysis several months after lesioning reveals that long-range horizontal connections projecting to scotomas from surrounding cortex are much denser than connections to non-scotoma V1. Sprouting of horizontal connections extending into scotomas might explain

how cells located there, initially silent after being deprived of their retinal input, acquire responses to the retinal input of surrounding regions of V1 (Darian-Smith and Gilbert, 1994; Arckens et al., 2000; Calford et al., 2003). Similar increases in horizontal connection density are found in somatosensory cortex after disruption of input, where functional reorganization is also observed (Merzenich, Kaas, Wall, Nelson et al., 1983; Calford and Tweedale, 1988; Pons et al., 1991; Florence et al., 1998).

The rate of bouton turnover found in this study (7 % per week), even in the absence of imposed learning or retinal lesions, indicates that synapses are added and removed completely, i.e., that connection plasticity can involve more than changes in the effectiveness of existing synapses. The turnover rate is surprisingly large, particularly if one considers the implications such a rate would have, if sustained and homogeneous over all boutons, for maintaining basic functional properties. If the total population of synapses is labile, functional stability could still be maintained by the directed formation of new connections that recapitulate the existing functional maps. Alternatively, it is possible that turnover involves only a particularly labile subset of synapses, which would then be responsible for

perceptual learning while the stable remainder mediates basic perceptual properties. Further work is needed to resolve this issue because the limited data at longer intervals presented here cannot strongly point to either possibility. Beyond the cortex in the normal adult, this issue is also relevant for how new neurons make appropriate connections in areas that undergo adult neurogenesis, such as mammalian hippocampus or in the bird song system, or when neural stem cells are introduced therapeutically to restore function in compromised brain areas.

2.5 EXPERIMENTAL PROCEDURES

2.5.1 ANIMAL PREPARATION AND VIRAL INJECTIONS

All AAV.EGFP injections and two-photon imaging sessions were carried out in anesthetized *Macaca fascicularis* monkeys and mice in accordance with institutional and federal guidelines for the treatment of animals. Under nembutal anesthesia and with monitoring of heart rate and breathing, an adult Macaque was secured in a stereotactic apparatus. Following scalp retraction, a small (2 mm × 5 mm) hole was drilled through the skull overlying V1, and an incision was made in the dura. Aliquots of

high-titer preparations of AAV.EGFP (80 nl containing 1.6×10^9 viral particles; capsid serotype 1) were pressured injected through glass micropipettes into superficial V1. Following viral injection, the scalp was sutured and the animal returned to its cage where it remained until imaging began at least 3 weeks later.

AAV.EGFP is a nonreplicative adeno-associated virus, the genes of which have been replaced by the gene encoding EGFP under control of the cytomegalovirus enhancer-promoter. AAV.EGFP vectors with three different capsid serotypes (1, 2, and 5) were tested. All imaged cells presented here were labeled with AAV.EGFP having a serotype 1 capsid. The virus was provided by Dr. Jean Bennett of the University of Pennsylvania and prepared as previously described (Xiao et al., 1999; Surace et al., 2003). The vectors were produced by transfection of 293 cells with three plasmids encoding (1) an EGFP expression cassette bearing the AAV serotype 2 inverted terminal repeats, (2) the AAV rep and cap genes, and (3) adenoviral helper function genes. The virus was subsequently purified through three successive centrifugations in CsCl gradients and titred using real-time PCR. AAV.EGFP is designed to minimize damage to

infected cells caused by viral function or an induced immune response. The only native viral sequences present in the vector's DNA payload are the inverted terminal repeats necessary for packaging of the DNA in the viral capsid. Lack of damage is evidenced by the consistently normal morphology (including axons; see Fig. 2.1A-2.1C for a 1 year interval) and density of labeled cells independent of time elapsed since the infection.

At the start of the first imaging session, the animal was fitted with a head-post. A custom-designed steel chamber that provided access for a microscope objective and that could be sealed between sessions was then fixed into place around the craniotomy using dental acrylic, and a larger (5–10 mm diameter) craniotomy was made surrounding the injection site. The dura was opened and retracted to expose an area of cortex ~6 mm in diameter. A quartz coverslip was then glued with surgical cyanoacrylate onto the edges of the opened dura. To maintain the clarity of the imaging window, the interior of the chamber was cleaned at the start of each imaging session and every 2 – 3 days otherwise. Animals were trained to sit in a restraint chair with their heads fixed so that the chamber could be cleaned on

a regular basis between imaging sessions. Cleaning included the stripping of connective tissue that quickly began to cover the pia within the craniotomy.

2.5.2 *IN VIVO* IMAGING

Two-photon imaging was performed using a Leica (Heidelberg, Germany) TCS Sp2 confocal microscope that was custom fitted with a moveable scanning head (W.D. et al., unpublished data). The head was fastened to a frame extending from the side of the standard scan unit (from which it received its excitation path) and could be moved in three dimensions using a Sutter (Novato, CA) MP-285-3Z micromanipulator and also rotated around one axis. This modification freed up the space surrounding the objective to provide easier placement with respect to the Macaque's skull chamber. Two-photon excitation (930 nm) was provided by a Ti-sapphire laser pumped by a 10 W frequency-doubled Nd:Vanadate Laser (Tsunami/Millenia system, Spectra Physics, Mountain View, CA).

During the first session, imaging began at the injection site. Subsequently, nearby regions of cortex containing EGFP-labeled axons were

identified and targeted for imaging on multiple occasions. Locating targeted regions within the chamber involved several steps. First, the identical pial vascular pattern could be seen in low-magnification images of the whole craniotomy and the higher-magnification superficial sections in two-photon Z stacks. Next, a microscopic grid affixed to a special chamber insert was placed in the chamber. The grid could be navigated with the microscope under reflected light more easily than the blood vessels and allowed placement of the objective with <100 μm resolution. After identifying a landmark in the vascular pattern where axons had previously been imaged, the objective could be directed to that spot under reflected light using the overlying grid.

Imaging was performed with a 40× water-immersion objective (Nikon FLUOR 40X/0.08W DIC M) which gave a 250 μm field of view. Scanning was done at a resolution (0.24 μm per pixel) sufficient to see fine axons and boutons. Stacks of optical sections were acquired at 1 μm z intervals. Despite the fastening of a coverslip over the exposed cortex to reduce movement, brain movement on the order of one to a few micrometers in all three dimensions sometimes occurred. Collected z sections, therefore, were

not always evenly spaced with regard to the tissue. The optical axis used for imaging was always perpendicular to the cortical surface, and any variation of imaging angle was likely to be within a few degrees. (It should also be noted that some specimen-orientation artifacts, if they exist, would not affect the main findings of the paper—complete loss or gain of en passant and terminaux boutons—because these changes are apparent regardless of the imaging angle.) To reconstruct axon projection zones over a larger area, we developed software to tile together numerous Z stacks. Imaging sessions of several hours provided imaged areas ~2 mm across.

Several pieces of evidence indicate that the boutonal dynamics we observed were not the result of phototoxicity associated with imaging. First, morphological parameters such as bouton size and average distance between boutons did not change between consecutive imaging sessions. Second, the rates of change of boutons were the same for the 1 week and 2 week intervals. Finally, differences in the frequency of imaging sessions (twice versus three times over a 2 week period) did not appear to influence the bouton turnover.

2.5.3 IMAGE ANALYSIS

Axons and boutons were identified and traced or marked by hand in the raw Z stacks of unprocessed two-photon images as well as stacks that had been processed with a Gaussian filter (1.5–2.0 pixel radius) to reduce noise. The examination of boutons involved multiple viewings of Z stacks at different brightness and contrast levels as well as different zoom levels to verify their relationship with flanking axon shafts. En passant boutons were identified as swellings along thinner axon shafts, terminaux boutons as swellings at the ends of thinner axonal branches. These swellings were not always symmetrically placed with respect to the shafts' axes. Before analyzing the axons imaged at multiple time points, we analyzed well-labeled axons from single time point *in vivo* imaging sessions as well as postmortem in slices and found that our method produced interbouton distance distributions that were highly consistent across the two data sets (Fig. 2.2) and that were similar to previously published findings (Amir et al., 1993; Braitenberg, 1998; Anderson et al., 2002).

This analysis yielded a population of en passant boutons that ranged from 0.5 to 1.5 μm in width and 0.5 to 2.2 μm in length. Average dimensions across the population (length = 1.2 ± 0.02 μm and width = 0.8 ± 0.01 μm) were larger than those calculated based upon studies employing electron microscopy (Mcguire et al., 1991; Peters et al., 1991; Ahmed et al., 1997; Schikorski and Stevens, 1999), presumably because of blurring in the optical images, with a minor contribution possible due to shrinkage during tissue processing for EM. Differences in brightness between imaging sessions were the main reason that axon segments had to be disregarded for analysis. A thin but imaging-impermeable layer of tissue constantly regrew over the pia in the area where the dura, which in the Macaque is an opaque barrier, had been removed. Removal of the regrown tissue re-exposed many, but not all, imaging targets. Potential artifacts resulting from changes in brightness across time points were avoided by comparing only those axon segments that had clearly discernible morphology at all time points for which the boutons were compared.

For the longitudinal analyses, the correspondence of individual boutons between imaging sessions was examined in order to determine

which boutons were stable over the full period and which boutons had appeared and disappeared within the period. A subset of axon segments was analyzed independently by two scorers. For each bouton, the scorers chose a confidence value of 1 to 4 to rate their certainty that the assignment was consistent with a set of agreed upon examples of boutons and non-boutons. The results of these analyses were similar overall and particularly so for the high-confidence assignments, which constituted the large majority of unchanged boutons and over half of the total number of reported losses and gains.

2.5.4 ACKNOWLEDGMENTS

The authors would like to thank Justin McManus for statistical analysis and helpful discussions; Jean Bennett for providing the virus; and Priya Gogia, Travis Hartman, Keith Hazleton, and Tina Marney for invaluable technical assistance. This work was performed with support of NIH grant EY 012896 and with funding from the Max-Planck Society. W.D. possesses a patent on two-photon technology. The other authors declare that they have no financial conflicts of interest pertaining to the content of this paper.

3 RAPID AXONAL SPROUTING AND PRUNING ACCOMPANY FUNCTIONAL REORGANIZATION IN PRIMARY VISUAL CORTEX

Homare Yamahachi[1], Sally A. Marik[1], Justin N. McManus[1], Winfried Denk[2] & Charles D. Gilbert[1]

1 Laboratory of Neurobiology, The Rockefeller University

2 Max Planck Institute for Medical Research, Heidelberg, Germany

3.1 SUMMARY

The cerebral cortex maintains a capacity for plastic change throughout life, both during normal processes of experience-dependent change, such as perceptual learning, and after functional recovery following CNS lesions or neurodegenerative disease. To study the mechanism of cortical plasticity at the level of circuitry, we used the topographic remapping that follows retinal lesions as a model system. Although it has been shown that sprouting and synaptogenesis of the intrinsic long-range horizontal connections formed by cortical pyramidal neurons within the lesion projection zone (LPZ) of

primary visual cortex are associated with the remapping, little is known about the dynamics of the process. To follow the same axons over time, before and after placing the lesions, we combined axonal labeling by viruses and *in vivo* two-photon microscope that enabled us to image identified neurons and their processes in the living Macaque brain. The virus was injected into locations that allowed us to image the horizontal projections to the LPZ. In the first few weeks following the retinal lesions, there was an exuberant outgrowth of axons projecting from the cortical area outside the LPZ towards the center of the LPZ. Over the subsequent two months, a parallel process of pruning of a subset of these axons was seen, resulting in a decline in axonal density in the LPZ. Overall there was a net increase in axonal density. Even those axons that project away from the LPZ showed increased turnover compared to a non-lesioned animal, although the axonal density was either stable or slightly reduced. These data indicate that the pattern of changes of the long-range horizontal connections parallel the changes in RF size and cortical topography over the weeks following retinal lesions. Furthermore, the sequence of exuberant sprouting followed by pruning represents a re-engagement of the program of synaptogenesis that occurs during early development.

3.2 INTRODUCTION

The cerebral cortex retains the capacity for experience-dependent changes throughout life. Experience-dependent plasticity in the adult primary visual cortex (V1) occurs during perceptual learning (Crist et al., 2001; Schoups et al., 2001; Li et al., 2004; 2006) or following altered sensory input resulting from CNS damage (Rose et al., 1960; Gilbert et al., 1990; Kaas et al., 1990; Heinen and Skavenski, 1991; Darian-Smith and Gilbert, 1994; Chino et al., 1995; Darian-Smith and Gilbert, 1995; Das and Gilbert, 1995; Calford et al., 2000; Mataga et al., 2004; Baker et al., 2005; Keck et al., 2008). When a circumscribed part of V1 is functionally deafferented by focal binocular retinal lesions, this area, known as the lesion projection zone (LPZ), is initially unresponsive to visual stimuli, but over time regains visually driven activity (Chino et al., 1992; Gilbert and Wiesel, 1992; Darian-Smith and Gilbert, 1995; Das and Gilbert, 1995). Some of these changes occur rapidly. Within hours following the lesion, the receptive fields (RFs) of the neurons inside the LPZ shift to parts of the retina surrounding the lesion (which we will refer to as the peri-LPZ). Over time, the recovery of visually driven activity and the associated remapping

of visual topography progress towards the center of the LPZ. The circuit underlying the reorganization is likely to involve the intrinsic long-range horizontal connections formed by the axone of cortical pyramidal cells. The extent of these connections matches the area of reorganization (Gilbert and Wiesel, 1979), and over longer periods of time (on the order of a year) following the lesion they undergo sprouting and synaptogenesis (Darian-Smith and Gilbert, 1994). Axonal sprouting could explain the recovery of visually driven activity of neurons inside the LPZ and the remapping of cortical topography occurring months after the lesion. The earlier studies were based on postmortem tracing of connections and comparisons of horizontal projections to the LPZ and to normal cortex. Now two-photon microscopy allows us to perform longitudinal studies of identified processes in the intact, living brain. The additional advantage of this approach is that it enables us to follow even rapid changes in cortical circuitry associated with the short-term changes in RFs and topography.

Two-photon microscopy has permitted the imaging of individual retinotectal axons (Ruthazer et al., 2006) and cortical axons during development (Portera-Cailliau et al., 2005), as well as in the adult brain (De

Paola et al., 2006; Majewska et al., 2006; Stettler et al., 2006) for extended periods of time. In the absence of any disruption of sensory input, boutons appear and disappear at a rate of 7 % per week, while axonal branching remains stable (Stettler et al., 2006). This observation was based on labeling of the axons by the delivery of genetically encoded fluorophores with viral vectors. With one such vector, AAV, we were able to induce long term, stable expression of the transgene in visual cortical neurons. Here, we combined two-photon imaging with these viral vectors to deliver the enhanced green fluorescent protein (EGFP) to specific neurons in V1 for longitudinal analysis of axon dynamics in V1 during the functional reorganization following retinal lesions.

3.3 RESULTS

To study the changes in cortical circuitry associated with retinal lesions, we combined electrophysiological mapping, labeling of the long-range horizontal connections with viral vectors, and two-photon microscopy in macaque primary visual cortex. The horizontal connections are formed by layer 2/3 cortical pyramidal neurons, and run for long distances parallel

to the cortical surface (on the order of 8mm). Because of their considerable length, they link neurons with widely separated RFs (Stettler et al., 2002), and are, therefore, good candidates for providing input from neurons with RFs outside the retinal lesion to neurons within the LPZ. The two-photon imaging technique (Denk et al., 1990) allowed us to do the necessary longitudinal studies, i.e. follow the same axons over time. We developed a preparation for chronic imaging of neuronal structure *in vivo* (Fig. 3.1). We used a genetically engineered, non-replicative adeno-associated virus (AAV) carrying the EGFP gene under the control of a CMV promoter. We made a series of injections of the virus into V1 along an antero-posterior axis, perpendicular to the V1/V2 border (Fig. 3.1B). EGFP expression was achieved in most of the neurons in a ~0.5mm radius around the injection site (covering an area of ~1 mm in diameter). We then waited for a period of at least two months for full expression of the transgene in the infected neurons. To prepare for imaging, we made a craniotomy over the opercular surface of V1 and inserted an artificial dura. This provided a window for imaging and inhibited overgrowth of the dura over the imaged area (see methods). Two areas of cortex were imaged, one medial and one lateral, approximately 1 mm from the injection sites. One of the imaged regions was within the

planned LPZ and the other within the surrounding peri-LPZ (Fig. 3.1B). It is important to note that the axons imaged in both regions originated from the same group of fluorescently labeled neurons. For each of the imaged regions, we collected 9 to 20 Z stacks, consisting of 100 images each, with 250 μm field of view, covering 200 μm in depth, and a total volume of 0.10 to 0.22 mm^3. On the day of making the retinal lesions, we first mapped the topography of the area of V1 under the craniotomy with extracellular recordings. This map provided the guide for making the lesions, which were placed so that their boundaries lay to the medial side of the virus injections, such that the infected neurons were located within the peri-LPZ, at ~1mm outside the LPZ. The lesions were placed at corresponding locations of the two retinas, so the LPZ would be completely devoid of retinal input immediately following the lesion (Fig. 3.1B). This allowed us to study axonal projections both into the LPZ and the peri-LPZ.

Figure 3.1. Experimental protocol

(A) Custom-built imaging chamber for long-term chronic *in vivo* imaging of axonal segments.

(B) Diagram showing the AAV-EGFP injections into V1 (green dots). The dashed rectangles indicate the areas imaged in the LPZ and the Peri-LPZ. The black dashed line indicates the border of the LPZ.

(C) Timeline of the experimental protocol.

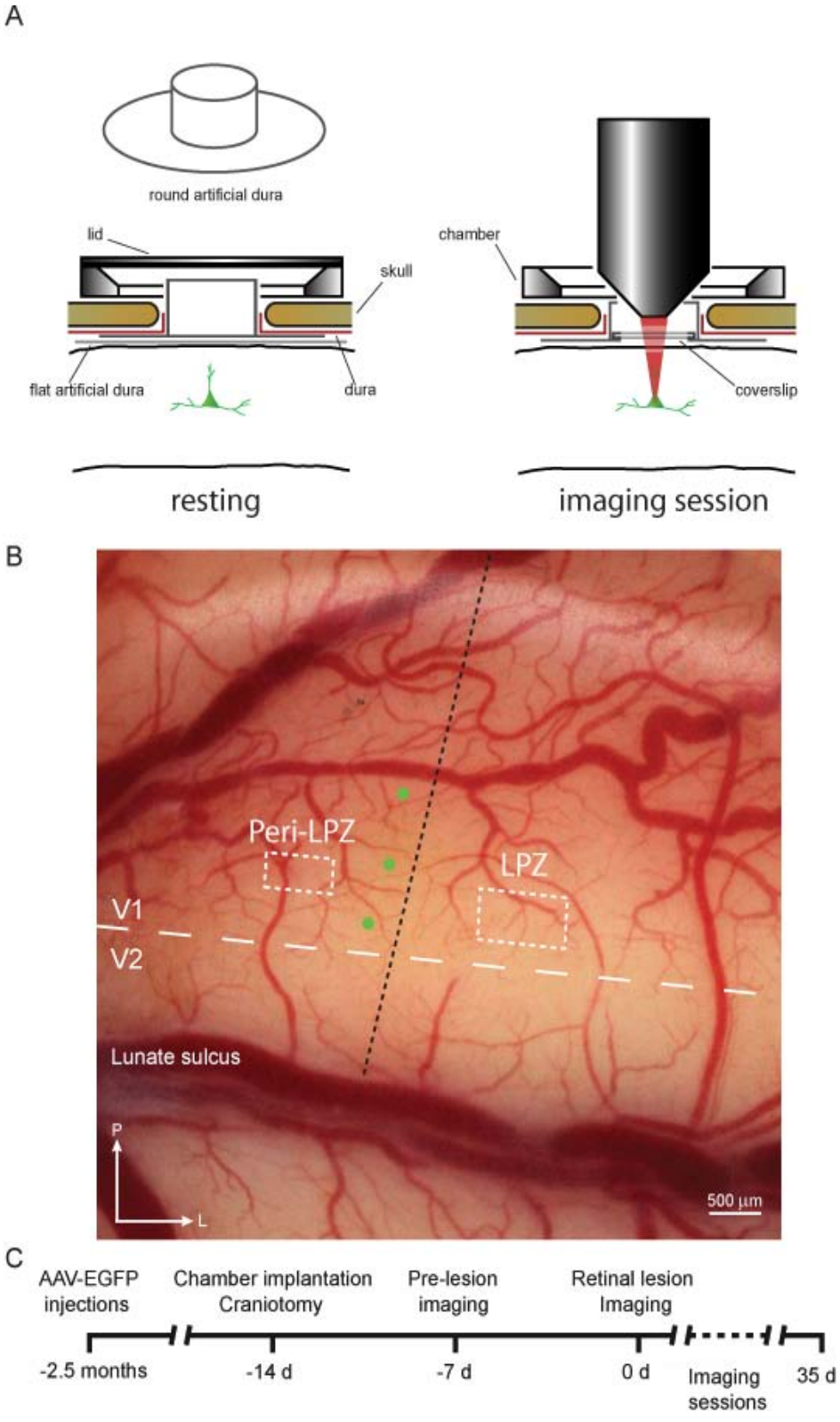
A
round artificial dura
lid
skull
flat artificial dura
dura
chamber
coverslip
resting
imaging session
B
Peri-LPZ
LPZ
V1
V2
Lunate sulcus
P
L
500 µm
C
AAV-EGFP injections
Chamber implantation Craniotomy
Pre-lesion imaging
Retinal lesion Imaging
-2.5 months
-14 d
-7 d
0 d
Imaging sessions
35 d

3.3.1 AXONAL DYNAMICS IN LPZ FOLLOWING BINOCULAR RETINAL LESIONS

Labeled axons within the LPZ and peri-LPZ cortex were imaged several times spanning a period of 7-8 weeks. For comparison between time points, we selected areas that provided clear images over the time period of interest. Axons were reconstructed using a semi-automatic tracing program (Neuromantic, www.rdg.ac.uk/neuromantic) to make 3D reconstructions of all the axons in the imaged areas. When comparing changes between regions, we reconstructed axons over the same cortical depths. To detect any appearance or disappearance of axon collaterals and boutons from week to week, we followed the same areas imaged at different time points. The same procedure was done for two animals. In the first animal (MA) there were several striking changes that began 5 hr after the lesion (Fig. 3.2 and 3.3). Firstly, the axon density increased markedly 5 hr after making the lesions, with an increment of 2.8 fold in density relative to the image taken one week prior (-7 d vs. 0 d, Fig. 3.3). The addition of axons (yellow fibers) was more pronounced toward the center of LPZ where the baseline density was quite sparse. Secondly, the massive increase in axon collaterals right

after the lesion was accompanied by a comparable extent of collateral elimination 14 days post-lesion (red fibers). Overall there was a net increase in axon density lasting the entire 28 days after the lesion ($p = 0.03$, compared to pre-lesion). The balance between axon addition and elimination changed over the following weeks. Addition peaked 5 hr after the lesion, then declined and stabilized after 14 days, at which point elimination peaked. The net effect over the entire period imaged (7 weeks) was an approximate doubling in axon density.

Figure 3.2. LPZ imaged 7 days before, 5 hr after, and 14 days after the lesion

Left, a projection of Z stacks to a depth of 150 μm show axonal segments. Right, reconstructions of axonal segments traced through the Z stacks. Note, how axon density increased markedly from the day of the lesion onward (0 d – 14 d). Streaking in the images is due to photomultiplier saturation.

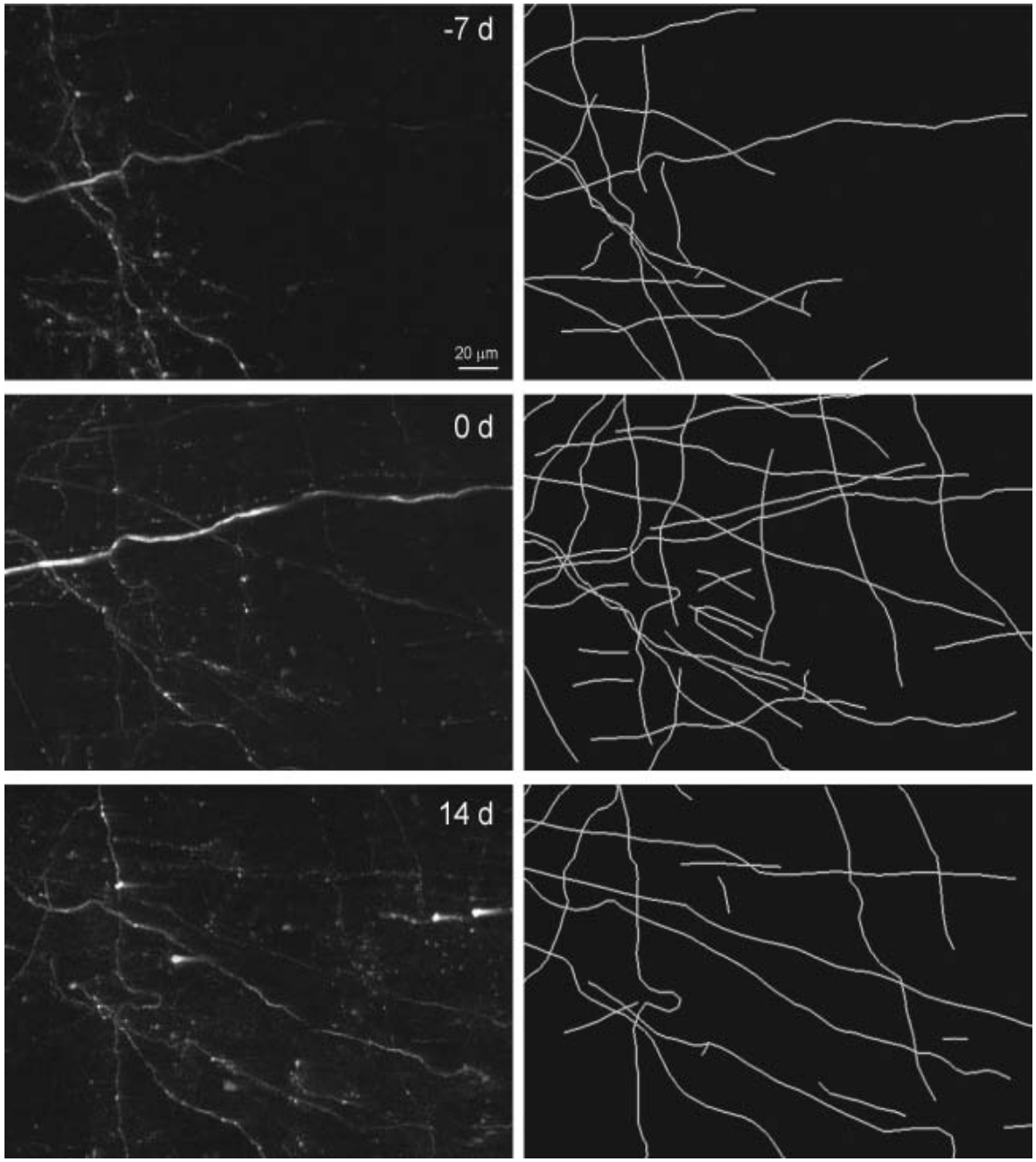
-7 d
20 µm
0 d
14 d

Figure 3.3. Axonal dynamics in LPZ (MA)

(A) Axonal tracing of Z stacks acquired through a depth of 200 μm. Grey: axon segments that remained unchanged compared to the previous time point; yellow: segments that were added; red: segments eliminated.

(B) Axon density (axonal length per unit of volume) for axons that had been added (yellow), pruned (red) and remained unchanged (gray) since the preceding imaging section. The total axon density is shown in black.

(C) Axon survival fraction. Axonal length still present from the initial axonal population (-7 d) as a fraction of the total initial length.

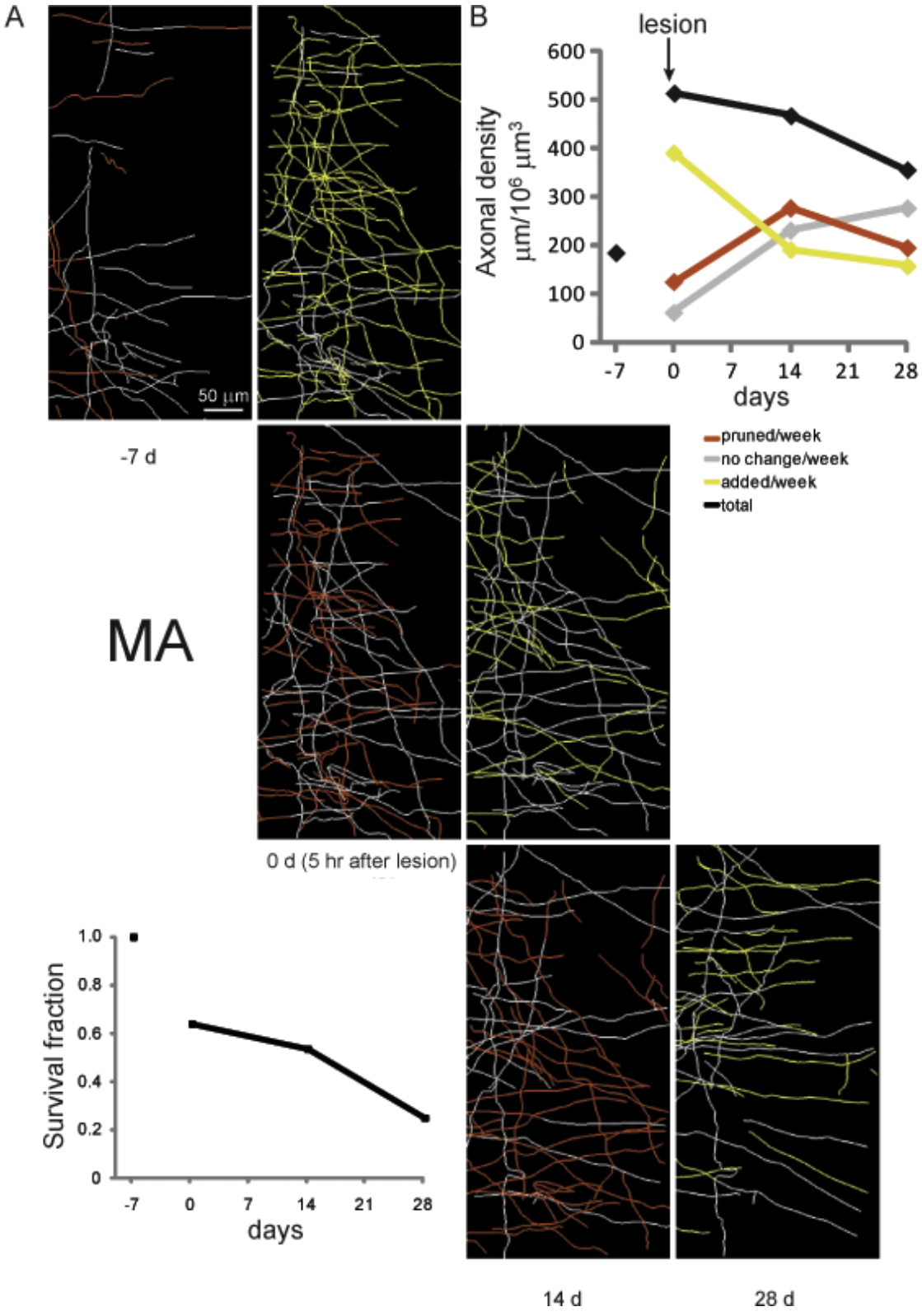
A
50 µm
-7 d
B
lesion
Axonal density
µm/10⁶ µm³
600
500
400
300
200
100
0
-7
0
7
14
21
28
days
pruned/week
no change/week
added/week
total
MA
0 d (5 hr after lesion)
Survival fraction
1.0
0.8
0.6
0.4
0.2
0
-7
0
7
14
21
28
days
14 d
28 d

The second animal (MB) showed the initial exuberant increase in axon density after the lesion (Fig. 3.4). This increase lasted the entire imaging session ($p = 0.03$, compared to pre-lesion). As with MA, the process was highly dynamic, with an active co-occurrence of axon addition and elimination, and the axon density was higher than pre-lesion at the end of the imaging period of 7 weeks (121 %). There were minor differences – for example, in MB compared to MA a higher fraction (46.8 % compared to 24.8 %) of axons present before the lesions were still present after 35 days (28 days for MA). Note also that in both animals the axons added following the lesion were more prone to be eliminated (the consecutive week-to-week changes ranged from 35 to 99% for axons that were added after the lesion vs. 6 to 53% for axons that were present before the lesion, $p = 0.02$).

Axons displayed several distinct retraction behaviors (Fig. 3.5). One example is an axon that existed at the time of the lesion and then at 14 days post-lesion, showed degenerative changes, including beading, swelling, retraction of short side branches, and detachment of axon fragments from their parent shaft (Fig. 3.5A). By day 28, this axon collateral had

disappeared completely. Another axon imaged from the day of the lesion (0 d) showed a progressive retraction of the axonal tip (Fig. 3.5B).

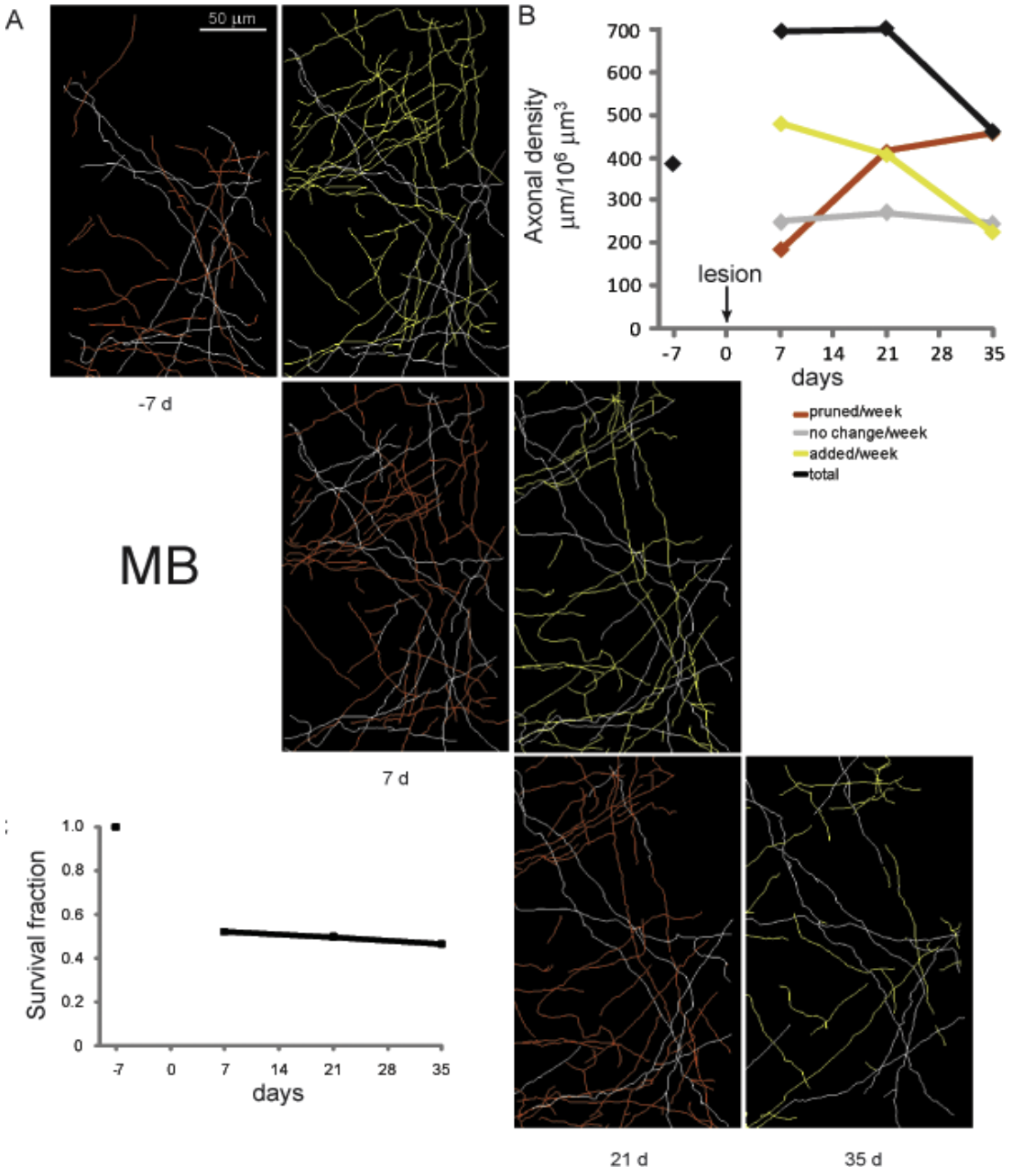

Figure 3.4. Axonal dynamics in LPZ in a second animal (MB)

Figure description exactly as for Figure 3.

Figure 3.5. Axon pruning modes

(A) An axon branch (arrow) present before (-7 d) and 5 hr after the lesion (0 d) undergoes degeneration by 14 d. Note the beading and swelling (*), and detachment of portions of axonal shaft (arrowhead).

By 28 d, remnants of the segment were no longer detected.

(B) Retraction of a terminal branch (arrow) is shown in a segment imaged from 0 d to 35 d.

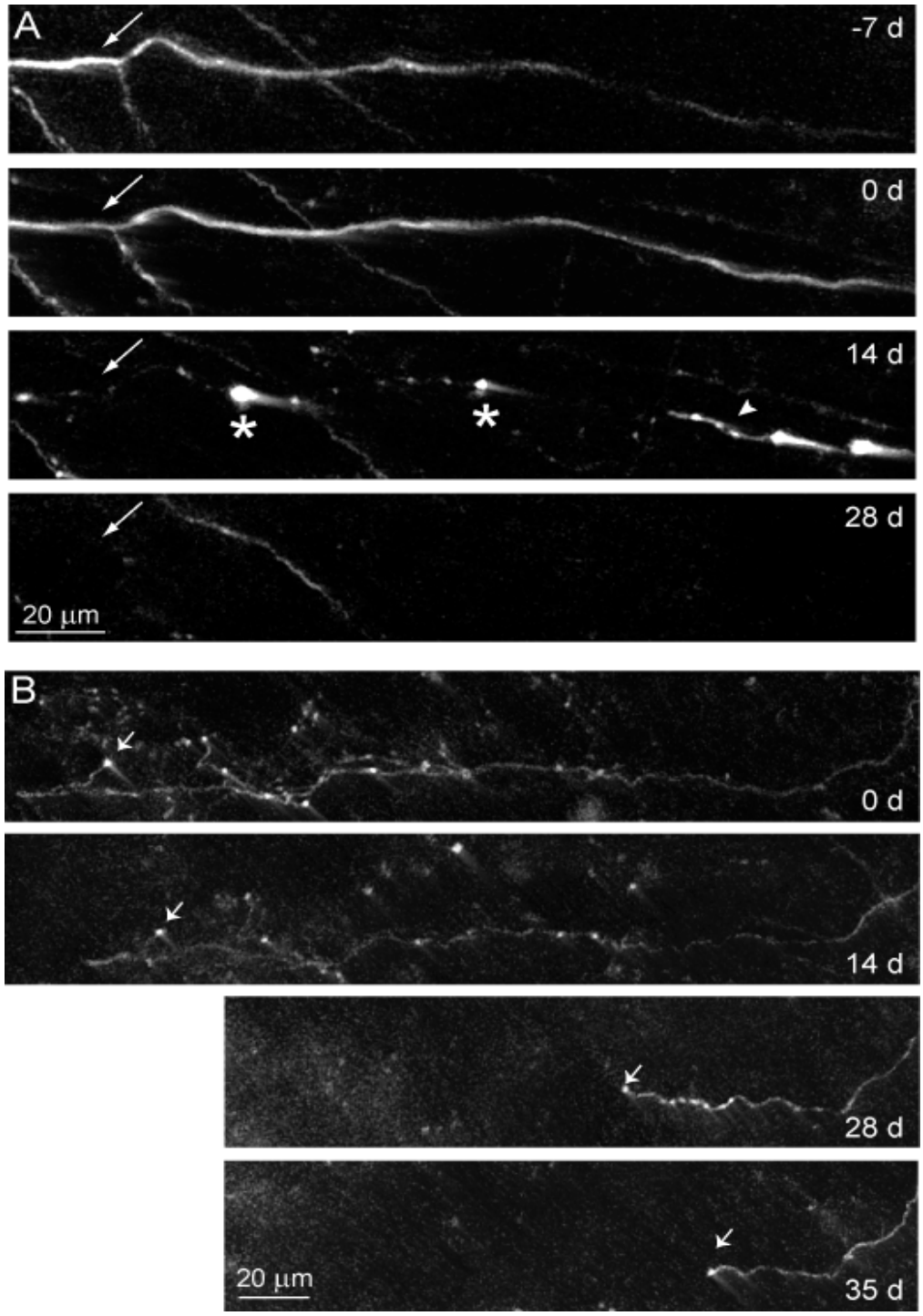
A
-7 d
0 d
14 d
28 d
20 µm
B
0 d
14 d
28 d
20 µm
35 d

3.3.2 AXONAL BOUTONS

In addition to the strikingly rapid turnover of axon branches, we also observed turnover of axonal boutons (on axons that were retained) that was substantially higher (peak rates of 72 % and 32 % per day for appearance and disappearance, respectively, for 17 axon segments totaling 1.24 mm in length, Fig. 3.6) than the baseline turnover rate (in non-lesioned animals) of ~7 % per week (Stettler et al., 2006). In the 28 days post-lesion, the percentage of boutons eliminated was higher than the addition (48.9 % vs. 15.6 %), resulting in a return of the bouton density to the level seen prior to the lesion (Fig. 3.6).

Figure 3.6. Bouton turnover in LPZ

(A) An axon segment showing an increase in bouton density immediately after the lesion (4 white arrows) and two being eliminated (yellow arrows).

(B) Bouton density.

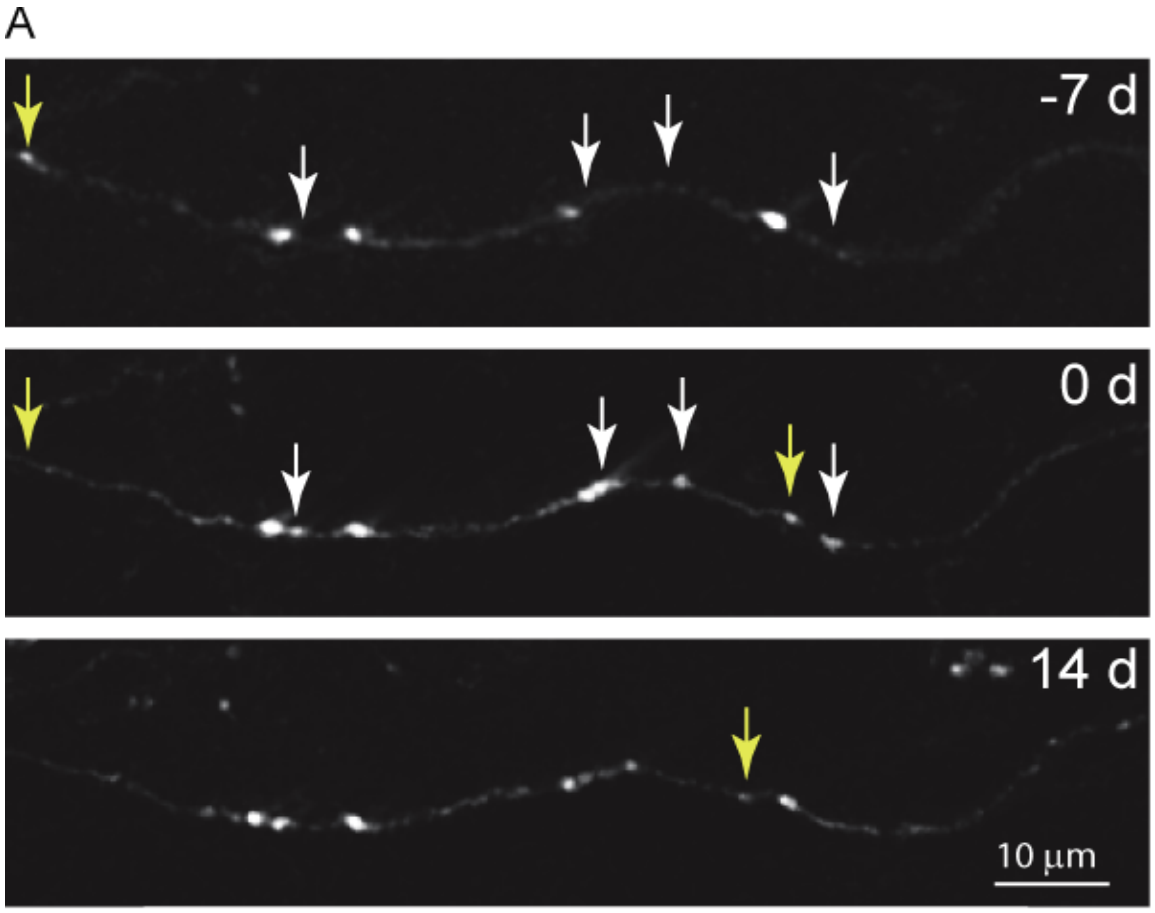
A
-7 d
0 d
14 d
10 µm

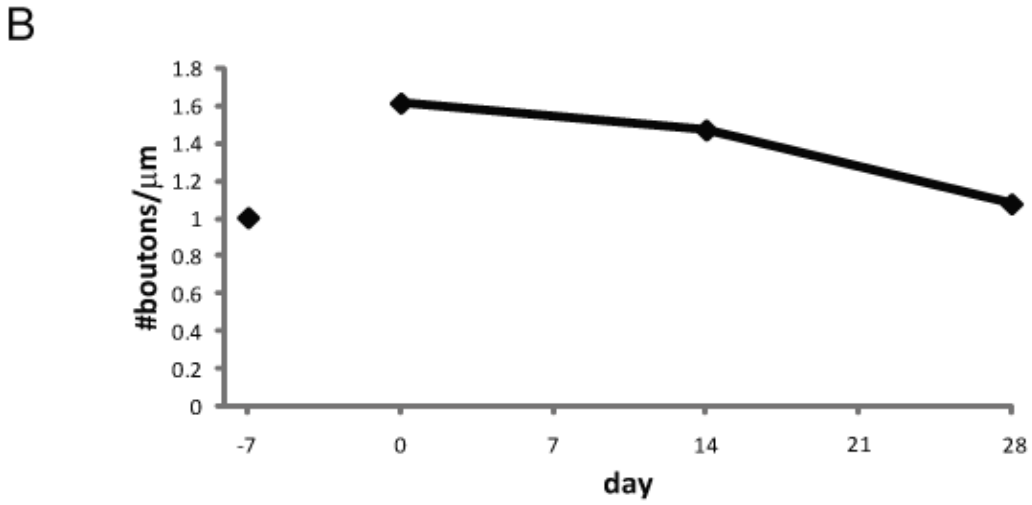
B
#boutons/µm
1.8
1.6
1.4
1.2
1
0.8
0.6
0.4
0.2
0
-7
0
7
14
21
28
day

3.3.3 AXONAL CHANGES IN THE PERI-LPZ

The axonal projections from the injection sites into the peri-LPZ showed a pattern of changes that was different from those seen in the LPZ, but also different from those in unlesioned animals. Without a lesion, the horizontal axon collaterals were stable, and underwent little sprouting or pruning, although there is substantial turnover of boutons (Stettler et al., 2006). With a lesion, we found, even in the peri-LPZ, axon addition and elimination, to be much more active, although with fewer additions in the peri-LPZ compared ($p = 0.03$) to the LPZ. In MA, although there was an elevation in both axonal sprouting and pruning, the rate of pruning was higher than the rate of addition (44 % vs. 27 %), and consequently there was a net reduction of 16.5 % in axon density after the lesion (Fig. 3.7). In the other animal, MB, following the lesions, the rates of sprouting and pruning were roughly in balance, so that there was no change in overall axon density over the time period of observation (Fig. 3.8). Both within the LPZ and peri-LPZ, therefore, retinal lesions triggered an immediate and a massive and highly dynamic program of axonal sprouting and pruning ultimately leading to lasting changes in axonal arbors, with a net increase in axon

density in the LPZ. In the peri-LPZ the density tended to either drop or remain the same.

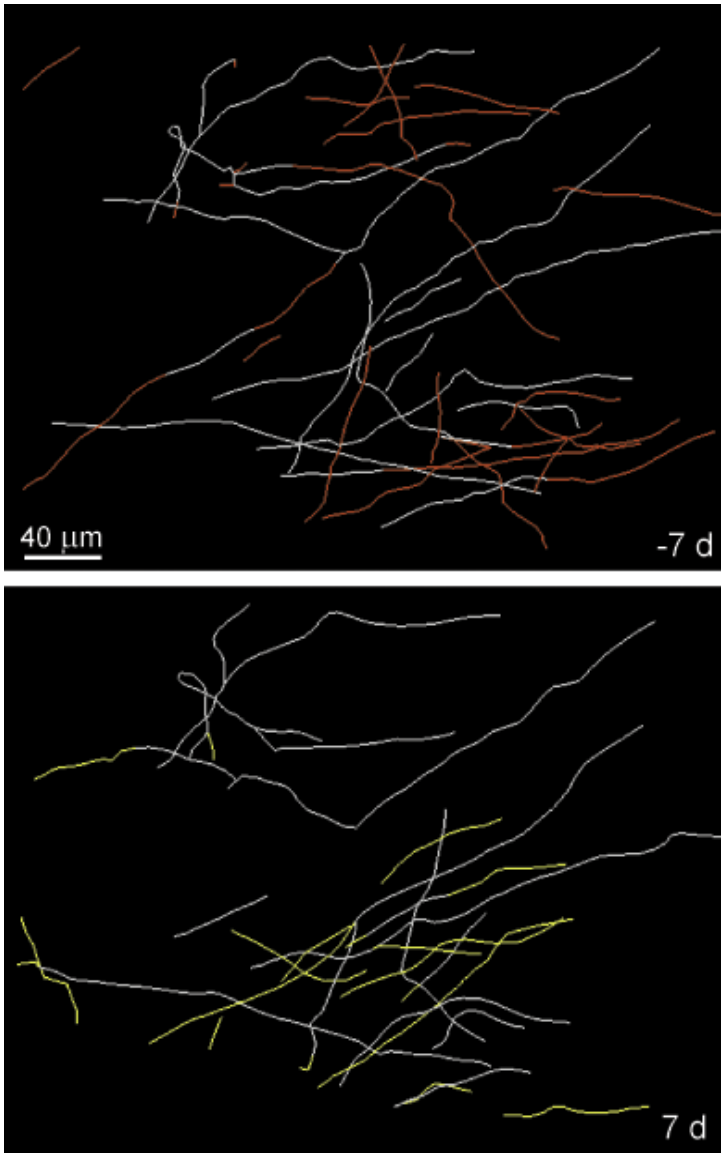

Figure 3.7. Axonal dynamics in Peri-LPZ (MA)

Axonal tracing of Z stacks acquired through a depth of 100 µm. In grey are represented axon segments that remained unchanged since the previous time point; segments that were added are in yellow; those eliminated in red.

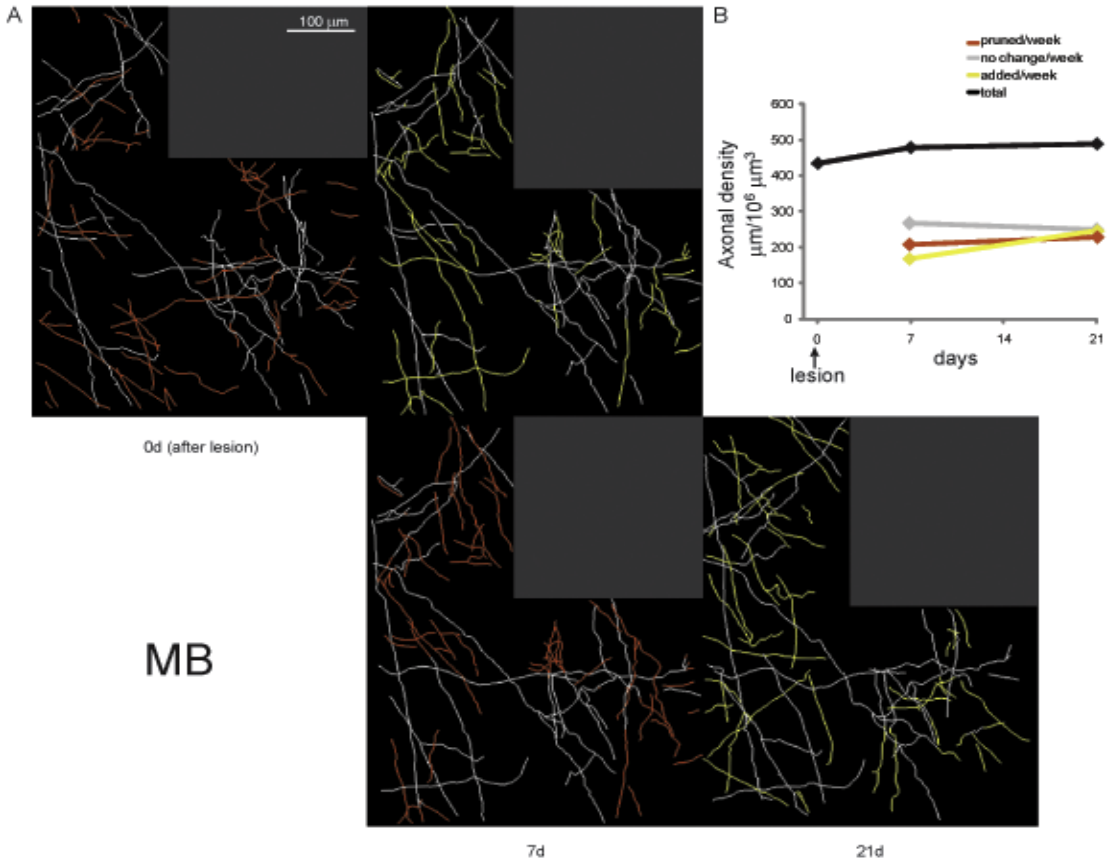

Figure 3.8. Axonal dynamics in Peri-LPZ (MB)

(A) Axonal tracing of Z stacks acquired through a depth of 100 µm. Axon segments that remained unchanged since to the previous time point are shown in gray; segments that were added are in yellow; those eliminated in red.

(B) Axon density represented as axonal length per unit of volume. Axon addition (yellow) and elimination (red) occurred at similar rates, resulting in a stable overall axon density (black).

3.4 DISCUSSION

After retinal lesions, the plexus of long-range horizontal axons showed remarkable changes beginning 5 hr after the lesions were made. These changes paralleled and are consistent with the alterations in RF position and size. Just as the RF changes begin as soon as the lesion is made, the sprouting of axon collaterals and proliferation of synaptic boutons is seen from the outset of the lesion. The RFs following the lesion are much larger than those seen in normal visual cortex, and over time they contract to normal size towards their new shifted cortical locations (Gilbert and Wiesel, 1992; Darian-Smith and Gilbert, 1995). Similarly, the horizontal axons proliferate at the highest rate within days of the lesion, with the density highest in the first week, then dropping due to an accelerated rate of axonal pruning. At the end of the observation interval, the axon density within the LPZ was still elevated.

3.4.1 AXONAL SPROUTING FOLLOWING RETINAL LESIONS

In the absence of retinal lesions, the plexus of horizontal axonal arbors is stable, but boutons are quite dynamic (De Paola et al., 2006; Stettler et al., 2006). This baseline of dynamic structural change may be what allows substantial morphological changes to begin immediately following alterations in visual experience. The model of focal binocular retinal lesions provides a window into the structural basis of experience-dependent cortical plasticity (Gilbert et al., 1990; Kaas et al., 1990; Heinen and Skavenski, 1991; Chino et al., 1995; Das and Gilbert, 1995; Calford et al., 2000; Giannikopoulos and Eysel, 2006; Keck et al., 2008). Initially the cortical region representing the area of the damaged retina is silenced, but over a period of minutes to months it recovers visually driven activity. The lack of reorganization at the level of lateral geniculate nucleus or of thalamocortical projections suggests that the topographic reorganization in V1 is due to changes in intra-cortical connectivity (Darian-Smith and Gilbert, 1995). Postmortem analysis of cortical connections 8 months following removal of sensory input showed that axonal sprouting of long-range horizontal connections made by pyramidal neurons in V1 accompanied functional

reorganization in adult striate cortex (Darian-Smith and Gilbert, 1994). Furthermore, the conservation of the pattern of orientation columns before the lesion and after recovery also supports the role of the pre-existing plexus of horizontal connections in the topographic reorganization (Das and Gilbert, 1995). This indicates that intercolumnar connections mediated by long-range horizontal axons, which under normal conditions play a modulatory role, develop a suprathreshold influence following recovery, leading to the shift in RF position for neurons in the LPZ. While previous studies could account for the long term changes in cortical topography occurring months after the lesion, the question arises as to how the rapid changes seen as early as on the day of the lesion could occur. One might have supposed that the immediate shift in RFs could be due to an increase in the effectiveness of existing synapses rather than the large scale sprouting observed at late time points. In the current study, however, we show that triggered by the retinal lesions, the neuronal circuitry can change dramatically in a matter of hours. A second observation afforded by our ability to follow the same axons *in vivo* over multiple time points is the dynamic nature of the change, involving a parallel sprouting and pruning. Although we still see a modest net increase in axonal density over the 6-7

week period of observation, this understates the massive amount of turnover of axons seen on a weekly basis. Initially the axon density increases ~2 fold. This amount of axonal arbor is pruned back at the longer time points, though still leaving a net increase. It is likely, given our previous results from much longer post-lesion periods, that the LPZ axons gradually continue to increase in density. At 6 months to 1 year following the lesion, the density of horizontal axon collaterals in the LPZ rises to a 2-fold increase relative to that seen in normal cortex (Darian-Smith and Gilbert, 1994).

It is informative to compare this efflorescence of axonal arbors with the time course of RF changes measured with electrophysiological recordings. The rapid change in the RFs of neurons just inside the LPZ (Gilbert and Wiesel, 1992), including shifts and RF expansion, parallels the short-term increase in axonal density. The subsequent contraction of RFs matches the observed decrease in the density of axons in the LPZ seen over the subsequent weeks. The final phase, of recovery completes the remapping of cortical topography, which progresses towards the center of the LPZ over long time periods, and includes the gradual build up of axon density in the LPZ.

Our data show that in response to retinal lesions, there is an initial exuberant outgrowth followed by a fine tuning of connections. This is reminiscent of the transient overproduction of axons and synapses that occur during development (Kasthuri and Lichtman, 2004; Neill et al., 2004). For example, geniculocortical arbors initially cover a large cortical territory during the first postnatal week, and then are refined to coalesce to form the basis of ocular dominance columns (Ferster and Levay, 1978; Levay and Stryker, 1979; Levay et al., 1980). Intra-cortical connections also show this process of refinement. The horizontal axon collaterals from pyramidal cells are initially fairly uniformly distributed at postnatal days 4 to 6, but by postnatal days 28 to 35 are selectively pruned and the remaining axons form enriched clusters of collaterals (Callaway and Katz, 1990).

While the rapidity of the changes observed here is unexpected, there is precedence for this rapidity of change. Several studies show that axons during development have the capability to undergo dramatic changes. Axonal arborization increases by 50 % over an 8 h period in *Xenopus* tadpoles (Witte et al., 1996) and cortical axons in postnatal mouse can gain up to 35 μm/hr or lose up to 25 μm/hr (Portera-Cailliau et al., 2005). During

a critical period in postnatal development experience causes rapid alterations in axonal arbors. Monocular deprivation for 6 to 7 days induces a gain in complexity of thalamocortical arbors serving the non-deprived eye, while the ones corresponding to the deprived eye show a gross reduction (Antonini and Stryker, 1993). Furthermore, the induction of divergent strabismus in kittens for only 2 d produces a rapid withdrawn of horizontal connections from opposite-eye columns in layer 2/3 (Trachtenberg and Stryker, 2001).

3.4.2 AXONAL DYNAMICS IN THE PERI-LPZ

Large-scale branching patterns remain unchanged in the adult cortex during normal experience (De Paola et al., 2006; Stettler et al., 2006). In contrast, we found that upon retinal lesions axons in the peri-LPZ are dynamic. Although axon density was maintained, axons were eliminated and added at a rate similar to that inside the LPZ. This suggests that the peri-LPZ is not equivalent to normal cortex in the absence of a retinal lesion. In fact, previous studies (Gilbert and Wiesel, 1992) suggest that the RF shifts are not limited to the LPZ but extend outward into the peri-LPZ. This effectively maintains optimal sampling of the remaining retinal space,

reflecting a process of de-correlation or maximal distancing of RF properties between neighboring neurons. The mechanism of this, at the level of circuitry, may be the destabilization of axon collaterals of peri-LPZ neurons that project both into the LPZ, which provides the signal that stimulates the process of axon turnover, and into the peri-LPZ. The difference observed between LPZ and peri-LPZ could be the newly available active postsynaptic sites in the LPZ, which are freed by the silencing of the direct interlaminar input and are taken over by the horizontal connections. This leads to the net increase in the density of horizontal collaterals in the LPZ, and not the peri-LPZ, which retains active interlaminar input.

The dramatic increase in axonal bouton density among retained axons following the lesion indicates that sensory deprivation altered the normal dynamics of bouton turnover (~7 % per week rate observed in normal cortex, De Paola et al., 2006 and Stettler et al., 2006). Instead of the rates of addition and elimination being balanced, more boutons were added initially than disappeared. The initial axonal exuberance in the LPZ is paralleled by the increase in bouton density. At later time points the densities of both axon collaterals and boutons return close to the values before the lesion,

although the axon density remains somewhat elevated. The increase in bouton turnover following alteration in visual experience complements findings in spine dynamics *in vivo* (Trachtenberg et al., 2002; Keck et al., 2008).

3.4.3 TWO FORMS OF AXON PRUNING: DEGENERATION AND RETRACTION

During development in the mouse, cortical neurons experience axonal retraction, in which the axonal tip retracts a few micrometers, and axonal degeneration, in which whole axonal segments are eliminated (Portera-Cailliau et al., 2005). We observed both types of pruning after the lesion. Short segments were retracted while whole branches were eliminated showing the characteristics of axons undergoing degeneration: enlargement and beading, followed by detachment from the main branch (Low and Cheng, 2005; Luo and O'leary, 2005; Low and Cheng, 2006). This is a further evidence that plasticity following sensory impairment in the adult recapitulates the developmental program. Our results demonstrate that the adult brain is capable of very rapid changes in circuitry following sensory

deprivation, and suggest that the fast remodeling of long-range horizontal connections accounts for the rapid functional reorganization of visual cortex observed from the onset of retinal lesions. This observation raises the possibility that similar circuit dynamic rewiring can occur under normal conditions and may underlie experience-dependent change in cortex, such as that associated with perceptual learning.

3.5 EXPERIMENTAL PROCEDURES

3.5.1 ANIMAL PREPARATION AND VIRAL INJECTIONS

All AAV.EGFP injections and two-photon imaging sessions were made under sterile conditions in two anesthetized adult primates (*Macaca fascicularis*) in accordance with institutional and federal guidelines for the treatment of animals.

Following initial induction of anesthesia with ketamine (10 mg/kg body weight), a venous cannula was inserted and the animal was intubated with an endotracheal tube. Anesthesia was maintained with pentobarbital (7 mg/kg/hr). The animal was placed in a stereotaxic apparatus. Heart rate and

breathing were monitored throughout the experiment. The scalp was retracted and a craniotomy of 5 mm x 15 mm was made overlying the V1/V2 border. The dura was opened and a high-titer preparation of adeno-associated virus (100 nl containing 1.6 x 10^9 viral particles) was pressure injected into the cortex (several pulses at 0.1 bar for 1 min, with 3-5 minutes resting period afterward) through borosilicate glass micropipettes (World Precision Instruments, Inc.) using a Picospritzer III (Parker Hannifin Corp.). AAV-EGFP was injected in V1 at a depth of 500 □m to label neurons with somata in layer 2/3. The AAV.EGFP was made as previously described (Stettler et al., 2006). After viral injection, a small piece of artificial dura (Tecoflex, Thermedics, Inc.) was positioned atop the cortex, the dura was sutured, the excised piece of bone was reinserted and secured with surgical cyanoacrylate (Vetbond, 3M), and the scalp wound was closed. After the surgery, the animal was returned to its cage where it remained until imaging began. Since the AAV strain used is nonreplicative, only those neurons that were infected during the viral injections will express EGFP.

At the start of the first imaging session, the animal was fitted with a head-post. A craniotomy ~16 mm in diameter was made to expose the dura

over the opercular surface, and a custom-designed stainless steel chamber was affixed to the bone over the craniotomy with dental acrylic (Perm Reline & Repair Resin, Coltène Whaledent, Inc.). Since the Macaque dura is opaque, it was removed prior to the first imaging session, along with the artificial dura inserted at the time of injection. This preparation allows approximately 2 months of two-photon imaging before the cortex is covered with a membrane that is impenetrable to focused infrared light. While overgrowth can be removed in the initial weeks, it eventually becomes adherent to the cortex and cannot be removed without damaging the cortical vasculature. To maximize the time over which we could obtain images following the retinal lesion, we restricted ourselves to two imaging sessions before lesion placement.

Tissue regrowth was minimized by the use of two dura substitutes while the animal was not being imaged (Fig. 3.1A, resting). A round flat artificial dura (EG-93A, Tecoflex Clear, Lubrizol Advanced Materials, Inc.) of 24 mm in diameter was placed on top of the cortex. A second pre-molded artificial dura (RTV615, Momentive Performance Materials, Inc.) place on top of the first one, consisted of a round sheet of 23 mm in diameter, on top

of which was a 13 mm external diameter ring, 1 mm thick and 7 mm high, which prevented the dura from growing into the center of the chamber (modified from Arieli et al., 2002). The chamber was then filled with 1.5 % agarose (Type IIIA, Sigma Aldrich Co). During imaging sessions both artificial duras were replaced by a single one similar to the second artificial dura, but with the bottom consisting of only a 12 mm glass coverslip (Warner Instruments, LLC) (Fig. 1, imaging session). In subsequent imaging sessions, the interior of the chamber was cleaned. This included the stripping of connective tissue covering the pia within the craniotomy.

3.5.2 *IN VIVO* IMAGING

Imaging was performed (largely as described in Stettler et al., 2006) using a custom-built microscope based on a Leica MP RS resonant microscope with a 40 X water-immersion objective (Nikon FLUOR 40X/0.8W DIC M). Two photon excitation (900-920 nm) was provided by a mode-locked Ti:sapphire laser pumped by a 10 W frequency-doubled Nd:Vanadate Laser (Tsunami/Millenia system, Spectra Physics). Imaging of EGFP used the following filter set: peak 525 nm, bandwidth 50 nm. Image

acquisition was controlled by Leica Confocal Software (Leica, Germany). To minimize cerebral movement artifacts while imaging, we designed a system that phased-locked the acquisition of images with the animal breathing cycle.

During the first session, imaging began by locating the injection sites using the vascular pattern on the brain surface as fiduciary marks. Subsequently, nearby regions of cortex containing EGFP-labeled axons were identified and targeted for imaging on multiple occasions. To specifically image long-range longitudinal projections from EGFP-labeled pyramidal neurons in V1, these regions were located 1.5 - 2 mm laterally and medially from the injection sites in V1. After each imaging session, the animal was put back in its cage to recover from the anesthesia.

3.5.3 MAPPING CORTICAL RFS AND RETINAL LESIONS

RFs were mapped as previously described (Darian-Smith and Gilbert, 1995). Briefly, a week after the initial imaging session, using insulated tungsten microelectrode (impedance 1-2 MΩ, Alpha Omega, Israel), evenly

spaced penetrations were made evenly spaced perpendicular to the cortical surface and restricted to the superficial layers. Recordings were not made in the areas already imaged to avoid possible artifacts due to microelectrode penetrations. At each location, RFs were mapped according to "minimum response" characteristics using a hand-held stimulator, and properties such as orientation selectivity and ocular dominance were noted. To minimize eye movement, the animals were paralyzed during mapping with a paralytic agent (vecuronium bromide, induction 60 ml/hr, maintenance 6 ml/hr).

Retinal lesions were made as described previously (Gilbert et al., 1990; Gilbert and Wiesel, 1992). Briefly, the electrode was returned to a location inside the boundaries of the desired site of the lesion. The lesion was placed to include an area that was either medial or lateral from the injection sites, and that had been already been imaged during the first imaging session. We localized the region of the retina corresponding to the recorded neuron using audio output from the electrode and a guide light from the ophthalmic laser (Iridex Corp.) as the visual stimulus. Visually driven activity from cortical neurons was thus used to guide the placement of the lesions. Once retinal lesions had been made in the appropriate locus,

cortical cells within the LPZ immediately became unresponsive to visual stimulation. Alterations in the response properties from neurons outside the LPZ were immediately documented after retinal lesions had been made and again, to confirm the extent of the lesion, before the second imaging session. Typically, the diode laser delivered 300 mW for 800 - 1000 msec.

3.5.4 IMAGE ANALYSIS

Axons were identified and traced by hand, with the aid of Neuromantic software (www.rdg.ac.uk/neuromantic/), in Z stacks that had been processed with a median filter to reduce noise (ImageJ, rsb.info.nih.gov/ij/). The semi-automated tracing of axons involved the examination in multiple viewings of Z stacks at different brightness and contrast levels as well as different zoom levels. Despite the use of the artificial dura and synchronizing the acquisition with the breathing cycle, brain movement on the order of one to a few micrometers in all three dimensions sometimes occurred. Therefore, we wrote an alignment program in Matlab (The MathWorks, Inc.) that translates each image in a 3D stack so that the cortical volume is reconstructed as accurately as possible. The program is constrained so that

only translations of each image in the X, Y, or Z directions are allowed (rotations and image warping are prohibited). First, the program automatically aligns all the images in a stack in the X-Y plane; second, it rearranges the images in the Z direction to ensure that adjacent images in the realigned stack correspond to adjacent cortical depths. The first step uses steepest descent minimization to find the lateral alignment of each image that minimizes the appearance of 'duplicated' axons and cell bodies in the maximum value Z projection of the stack. The second step shuffles the realigned image slices to find the appropriate depth for each image that maximizes the similarity of adjacent slices over the whole stack. Importantly, the program features a graphical user interface that allows the user to manually and interactively modify the results from the automatic X-Y and Z alignments. The user intervention reduces the susceptibility of the program to local minima and ensures that the alignments are appropriate. We compared the data using χ^2 test.

4 BIBLIOGRAPHY

AHMED, B. *et al.* (1997). Map of the synapses onto layer 4 basket cells of the primary visual cortex of the cat. J Comp Neurol *380*, 230-42.

ALSINA, B. *et al.* (2001). Visualizing synapse formation in arborizing optic axons *in vivo*: dynamics and modulation by BDNF. Nat Neurosci *4*, 1093-101.

AMIR, Y. *et al.* (1993). Cortical hierarchy reflected in the organization of intrinsic connections in macaque monkey visual cortex. J Comp Neurol *334*, 19-46.

ANDERSON, J. C. *et al.* (2002). Chance or design? Some specific considerations concerning synaptic boutons in cat visual cortex. J Neurocytol *31*, 211-29.

ANDERSON, J. C. *et al.* (1998). The connection from cortical area V1 to V5: a light and electron microscopic study. J Neurosci *18*, 10525-40.

ANDERSON, J. C. *et al.* (1994). Synaptic output of physiologically identified spiny stellate neurons in cat visual cortex. J Comp Neurol *341*, 16-24.

ANDERSON, J. C.; MARTIN, K. A. (2001). Does bouton morphology optimize axon length? Nat Neurosci *4*, 1166-7.

ANDERSON, J. C.; MARTIN, K. A. (2005). Connection from cortical area V2 to V3 A in macaque monkey. J Comp Neurol *488*, 320-30.

ANTONINI, A.; STRYKER, M. P. (1993a). Development of individual geniculocortical arbors in cat striate cortex and effects of binocular impulse blockade. J Neurosci *13*, 3549-73.

ANTONINI, A.; STRYKER, M. P. (1993b). Rapid remodeling of axonal arbors in the visual cortex. Science *260*, 1819-21.

ARCKENS, L. *et al.* (2000). Cooperative changes in GABA, glutamate and activity levels: the missing link in cortical plasticity. Eur J Neurosci *12*, 4222-32.

ARIELI, A. *et al.* (2002). Dural substitute for long-term imaging of cortical activity in behaving monkeys and its clinical implications. J Neurosci Methods *114*, 119-33.

BAKER, C. I. *et al.* (2005). Reorganization of visual processing in macular degeneration. J Neurosci *25*, 614-8.

BALICE-GORDON, R. J.; LICHTMAN, J. W. (1990). *In vivo* visualization of the growth of pre- and postsynaptic elements of neuromuscular junctions in the mouse. J Neurosci *10*, 894-908.

BARTLETT, J. S. *et al.* (1998). Selective and rapid uptake of adeno-associated virus type 2 in brain. Hum Gene Ther *9*, 1181-6.

BEN-SHAHAR, O. *et al.* (2003). Cortical connections and early visual function: intra- and inter-columnar processing. J Physiol Paris *97*, 191-208.

BENNETT, J. *et al.* (1999). Stable transgene expression in rod photoreceptors after recombinant adeno-associated virus-mediated gene transfer to monkey retina. Proc Natl Acad Sci U S A *96*, 9920-5.

BHATT, D. H. *et al.* (2004). Cyclic AMP-induced repair of zebrafish spinal circuits. Science *305*, 254-8.

BISHOP, D. L. *et al.* (2004). Axon branch removal at developing synapses by axosome shedding. Neuron *44*, 651-61.

BLASDEL, G. G. *et al.* (1985). Intrinsic connections of macaque striate cortex: axonal projections of cells outside lamina 4C. J Neurosci *5*, 3350-69.

BOSKING, W. H. *et al.* (1997). Orientation selectivity and the arrangement of horizontal connections in tree shrew striate cortex. J Neurosci *17*, 2112-27.

BRAITENBERG, V. (1998). Selection, the impersonal engineer. Artif Life *4*, 309-10.

BUFFELLI, M. *et al.* (2003). Genetic evidence that relative synaptic efficacy biases the outcome of synaptic competition. Nature *424*, 430-4.

BURKE, W. (1999). Psychophysical observations concerned with a foveal lesion (macular hole). Vision Res *39*, 2421-7.

CALFORD, M. B.; TWEEDALE, R. (1988). Immediate and chronic changes in responses of somatosensory cortex in adult flying-fox after digit amputation. Nature *332*, 446-8.

CALFORD, M. B. *et al.* (2000). Plasticity in adult cat visual cortex (area 17) following circumscribed monocular lesions of all retinal layers. J Physiol *524 Pt 2*, 587-602.

CALFORD, M. B. *et al.* (2003). Topographic plasticity in primary visual cortex is mediated by local corticocortical connections. J Neurosci *23*, 6434-42.

CALLAWAY, E. M.; KATZ, L. C. (1990). Emergence and refinement of clustered horizontal connections in cat striate cortex. J Neurosci *10*, 1134-53.

CHAMBERLIN, N. L. *et al.* (1998). Recombinant adeno-associated virus vector: use for transgene expression and anterograde tract tracing in the CNS. Brain Res *793*, 169-75.

CHANG, F. L.; GREENOUGH, W. T. (1982). Lateralized effects of monocular training on dendritic branching in adult split-brain rats. Brain Res *232*, 283-92.

CHEN, C.; REGEHR, W. G. (2000). Developmental remodeling of the retinogeniculate synapse. Neuron *28*, 955-66.

CHINO, Y. M. (1999). The role of visual experience in the cortical topographic map reorganization following retinal lesions. Restor Neurol Neurosci *15*, 165-76.

CHINO, Y. M. *et al.* (1992). Rapid reorganization of cortical maps in adult cats following restricted deafferentation in retina. Vision Res *32*, 789-96.

CHINO, Y. M. *et al.* (1995). Receptive-field properties of deafferentated visual cortical neurons after topographic map reorganization in adult cats. J Neurosci *15*, 2417-33.

CHINO, Y. M. *et al.* (1991). Disruption of binocularly correlated signals alters the postnatal development of spatial properties in cat striate cortical neurons. J Neurophysiol *65*, 841-59.

CHISUM, H. J.; FITZPATRICK, D. (2004). The contribution of vertical and horizontal connections to the receptive field center and surround in V1. Neural Netw *17*, 681-93.

CHISUM, H. J. *et al.* (2003). Emergent properties of layer 2/3 neurons reflect the collinear arrangement of horizontal connections in tree shrew visual cortex. J Neurosci *23*, 2947-60.

CHKLOVSKII, D. B. *et al.* (2004). Cortical rewiring and information storage. Nature *431*, 782-8.

COHEN-CORY, S.; FRASER, S. E. (1995). Effects of brain-derived neurotrophic factor on optic axon branching and remodelling *in vivo*. Nature *378*, 192-6.

COLMAN, H. *et al.* (1997). Alterations in synaptic strength preceding axon withdrawal. Science *275*, 356-61.

CRAIK, K. J. W. (1966). On the effects of looking at the sun. In: The Nature of Psychology, edited by Sherwood S. L. CambridgeL Cambridge University Press.

CRIST, R. E. *et al.* (1997). Perceptual learning of spatial localization: specificity for orientation, position, and context. J Neurophysiol *78*, 2889-94.

CRIST, R. E. *et al.* (2001). Learning to see: experience and attention in primary visual cortex. Nat Neurosci *4*, 519-25.

DARIAN-SMITH, C.; GILBERT, C. D. (1994). Axonal sprouting accompanies functional reorganization in adult cat striate cortex. Nature *368*, 737-40.

DARIAN-SMITH, C.; GILBERT, C. D. (1995). Topographic reorganization in the striate cortex of the adult cat and monkey is cortically mediated. J. Neurosci. *15*, 1631-1647.

DAS, A.; GILBERT, C. D. (1995). Long-range horizontal connections and their role in cortical reorganization revealed by optical recording of cat primary visual cortex. Nature *375*, 780-4.

DE PAOLA, V. *et al.* (2003). AMPA receptors regulate dynamic equilibrium of presynaptic terminals in mature hippocampal networks. Nat Neurosci *6*, 491-500.

DE PAOLA, V. *et al.* (2006). Cell type-specific structural plasticity of axonal branches and boutons in the adult neocortex. Neuron *49*, 861-75.

DENK, W. *et al.* (1990). Two-photon laser scanning fluorescence microscopy. Science *248*, 73-6.

DENK, W.; SVOBODA, K. (1997). Photon upmanship: why multiphoton imaging is more than a gimmick. Neuron *18*, 351-7.

DITTGEN, T. *et al.* (2004). Lentivirus-based genetic manipulations of cortical neurons and their optical and electrophysiological monitoring *in vivo*. Proc Natl Acad Sci U S A *101*, 18206-11.

DREHER, B. *et al.* (2001). Cortical plasticity revealed by circumscribed retinal lesions or artificial scotomas. Prog Brain Res *134*, 217-46.

EHRENGRUBER, M. U. *et al.* (2001). Gene transfer into neurons from hippocampal slices: comparison of recombinant Semliki Forest Virus, adenovirus, adeno-associated virus, lentivirus, and measles virus. Mol Cell Neurosci *17*, 855-71.

EYSEL, U. T. *et al.* (1980). A functional sign of reorganization in the visual system of adult cats: lateral geniculate neurons with displaced receptive fields after lesions of the nasal retina. Brain Res *181*, 285-300.

EYSEL, U. T. *et al.* (1981). Late spreading of excitation in the lateral geniculate nucleus following visual deafferentation is independent of the size of retinal lesions. Brain Res *204*, 189-93.

FELDMEYER, D. *et al.* (2002). Synaptic connections between layer 4 spiny neurone-layer 2/3 pyramidal cell pairs in juvenile rat barrel cortex: physiology and anatomy of interlaminar signalling within a cortical column. J Physiol *538*, 803-22.

FENDICK, M.; WESTHEIMER, G. (1983). Effects of practice and the separation of test targets on foveal and peripheral stereoacuity. Vision Res *23*, 145-50.

FERSTER, D.; LEVAY, S. (1978). The axonal arborizations of lateral geniculate neurons in the striate cortex of the cat. J Comp Neurol *182*, 923-44.

FLANAGAN-STEET, H. *et al.* (2005). Neuromuscular synapses can form *in vivo* by incorporation of initially aneural postsynaptic specializations. Development *132*, 4471-81.

FLORENCE, S. L. *et al.* (1998). Large-scale sprouting of cortical connections after peripheral injury in adult macaque monkeys. Science *282*, 1117-21.

FOA, L. *et al.* (2001). The scaffold protein, Homer1b/c, regulates axon pathfinding in the central nervous system in vivo. Nat Neurosci *4*, 499-506.

FRIEDLANDER, M. J. *et al.* (1991). Effects of monocular visual deprivation on geniculocortical innervation of area 18 in cat. J Neurosci *11*, 3268-88.

GAN, W. B. *et al.* (2003). Synaptic dynamism measured over minutes to months: age-dependent decline in an autonomic ganglion. Nat Neurosci *6*, 956-60.

GAN, W. B.; LICHTMAN, J. W. (1998). Synaptic segregation at the developing neuromuscular junction. Science *282*, 1508-11.

GERRITS, H. J.; TIMMERMAN, G. J. (1969). The filling-in process in patients with retinal scotomata. Vision Res *9*, 439-42.

GIANNIKOPOULOS, D. V.; EYSEL, U. T. (2006). Dynamics and specificity of cortical map reorganization after retinal lesions. Proc Natl Acad Sci U S A *103*, 10805-10.

GILBERT, C. D. (1998). Adult cortical dynamics. Physiol Rev *78*, 467-85.

GILBERT, C. D. *et al.* (1996). Spatial integration and cortical dynamics. Proc Natl Acad Sci U S A *93*, 615-22.

GILBERT, C. D. *et al.* (1990). Lateral interactions in visual cortex. Cold Spring Harb Symp Quant Biol *55*, 663-77.

GILBERT, C. D. *et al.* (2001). The neural basis of perceptual learning. Neuron *31*, 681-97.

GILBERT, C. D.; WIESEL, T. N. (1979). Morphology and intracortical projections of functionally characterised neurones in the cat visual cortex. Nature *280*, 120-5.

GILBERT, C. D.; WIESEL, T. N. (1983). Clustered intrinsic connections in cat visual cortex. J Neurosci *3*, 1116-33.

GILBERT, C. D.; WIESEL, T. N. (1989). Columnar specificity of intrinsic horizontal and corticocortical connections in cat visual cortex. J Neurosci *9*, 2432-42.

GILBERT, C. D.; WIESEL, T. N. (1990). The influence of contextual stimuli on the orientation selectivity of cells in primary visual cortex of the cat. Vision Res *30*, 1689-701.

GILBERT, C. D.; WIESEL, T. N. (1992). Receptive field dynamics in adult primary visual cortex. Nature *356*, 150-2.

GOEPPERT-MAYER, M. (1931). Ueber Elementarakte mit zwei Quantenspruengen. Ann. Phys. *9*, 273.

GRUTZENDLER, J. *et al.* (2002). Long-term dendritic spine stability in the adult cortex. Nature *420*, 812-6.

HARRIS, K. M.; SULTAN, P. (1995). Variation in the number, location and size of synaptic vesicles provides an anatomical basis for the nonuniform probability of release at hippocampal CA1 synapses. Neuropharmacology *34*, 1387-95.

HEINEN, S. J.; SKAVENSKI, A. A. (1991). Recovery of visual responses in foveal V1 neurons following bilateral foveal lesions in adult monkey. Exp Brain Res *83*, 670-4.

HERING, H.; SHENG, M. (2001). Dendritic spines: structure, dynamics and regulation. Nat Rev Neurosci *2*, 880-8.

HIRSCH, J. A.; GILBERT, C. D. (1991). Synaptic physiology of horizontal connections in the cat's visual cortex. J Neurosci *11*, 1800-9.

HOLTMAAT, A. J. *et al.* (2005). Transient and persistent dendritic spines in the neocortex *in vivo*. Neuron *45*, 279-91.

HU, B. *et al.* (2005). BDNF stabilizes synapses and maintains the structural complexity of optic axons *in vivo*. Development *132*, 4285-98.

HUA, J. Y. *et al.* (2005). Regulation of axon growth *in vivo* by activity-based competition. Nature *434*, 1022-6.

HUBEL, D. H.; WIESEL, T. N. (1962). Receptive fields, binocular interaction and functional architecture in the cat's visual cortex. J Physiol *160*, 106-54.

HUBEL, D. H.; WIESEL, T. N. (1968). Receptive fields and functional architecture of monkey striate cortex. J Physiol *195*, 215-43.

HUBEL, D. H.; WIESEL, T. N. (1970). The period of susceptibility to the physiological effects of unilateral eye closure in kittens. J Physiol *206*, 419-36.

HUBEL, D. H.; WIESEL, T. N. (1977). Ferrier lecture. Functional architecture of macaque monkey visual cortex. Proc R Soc Lond B Biol Sci *198*, 1-59.

HUBEL, D. H. *et al.* (1977). Plasticity of ocular dominance columns in monkey striate cortex. Philos Trans R Soc Lond B Biol Sci *278*, 377-409.

ITO, M.; GILBERT, C. D. (1999). Attention modulates contextual influences in the primary visual cortex of alert monkeys. Neuron *22*, 593-604.

JAVAHERIAN, A.; CLINE, H. T. (2005). Coordinated motor neuron axon growth and neuromuscular synaptogenesis are promoted by CPG15 *in vivo*. Neuron *45*, 505-12.

JOHNSON, F. A. *et al.* (1999). Activity-dependent refinement in the goldfish retinotectal system is mediated by the dynamic regulation of processes withdrawal: an *in vivo* imaging study. J Comp Neurol *406*, 548-62.

JONTES, J. D. *et al.* (2000). Growth cone and dendrite dynamics in zebrafish embryos: early events in synaptogenesis imaged *in vivo*. Nat Neurosci *3*, 231-7.

KAAS, J. H. *et al.* (1990). Reorganization of retinotopic cortical maps in adult mammals after lesions of the retina. Science *248*, 229-31.

KALASKA, J.; POMERANZ, B. (1979). Chronic paw denervation causes an age-dependent appearance of novel responses from forearm in "paw cortex" of kittens and adult cats. J Neurophysiol *42*, 618-33.

KAPADIA, M. K. *et al.* (1995). Improvement in visual sensitivity by changes in local context: parallel studies in human observers and in V1 of alert monkeys. Neuron *15*, 843-56.

KAPADIA, M. K. *et al.* (2000). Spatial distribution of contextual interactions in primary visual cortex and in visual perception. J Neurophysiol *84*, 2048-62.

KAPLITT, M. G. *et al.* (1994). Long-term gene expression and phenotypic correction using adeno-associated virus vectors in the mammalian brain. Nat Genet *8*, 148-54.

KARNI, A.; SAGI, D. (1991). Where practice makes perfect in texture discrimination: evidence for primary visual cortex plasticity. Proc Natl Acad Sci U S A *88*, 4966-70.

KASTHURI, N.; LICHTMAN, J. W. (2003). The role of neuronal identity in synaptic competition. Nature *424*, 426-30.

KASTHURI, N., LICHTMAN, J. W. (2004). Structural dynamics of synapses in living animals. Curr Opin Neurobiol *14*, 105-111.

KECK, T. *et al.* (2008). Massive restructuring of neuronal circuits during functional reorganization of adult visual cortex. Nat Neurosci *11*, 1162-7.

KELLER, A.; ASANUMA, H. (1993). Synaptic relationships involving local axon collaterals of pyramidal neurons in the cat motor cortex. J Comp Neurol *336*, 229-42.

KERSCHENSTEINER, M. *et al.* (2005). *In vivo* imaging of axonal degeneration and regeneration in the injured spinal cord. Nat Med *11*, 572-7.

KINCAID, A. E. *et al.* (1998). Connectivity and convergence of single corticostriatal axons. J Neurosci *18*, 4722-31.

KISVARDAY, Z. F.; EYSEL, U. T. (1993). Functional and structural topography of horizontal inhibitory connections in cat visual cortex. Eur J Neurosci *5*, 1558-72.

KISVARDAY, Z. F. *et al.* (1986). Synaptic targets of HRP-filled layer III pyramidal cells in the cat striate cortex. Exp Brain Res *64*, 541-52.

KNOTT, G. W. *et al.* (2002). Formation of dendritic spines with GABAergic synapses induced by whisker stimulation in adult mice. Neuron *34*, 265-73.

LEVAY, S.; STRYKER, M. P. (1979). The development of ocular dominance columns in the cat. Soc. Neurosci. Symp. *4*.

LEVAY, S. *et al.* (1980). The development of ocular dominance columns in normal and visually deprived monkeys. J Comp Neurol *191*, 1-51.

LI, W.; GILBERT, C. D. (2002). Global contour saliency and local colinear interactions. J Neurophysiol *88*, 2846-56.

LI, W. *et al.* (2004). Perceptual learning and top-down influences in primary visual cortex. Nat Neurosci *7*, 651-7.

LI, W. *et al.* (2006). Contour saliency in primary visual cortex. Neuron *50*, 951-62.

LICHTMAN, J. W. *et al.* (1987). Visualization of neuromuscular junctions over periods of several months in living mice. J Neurosci *7*, 1215-22.

LIU, Y.; HALLORAN, M. C. (2005). Central and peripheral axon branches from one neuron are guided differentially by Semaphorin3D and transient axonal glycoprotein-1. J Neurosci *25*, 10556-63.

LOW, L. K.; CHENG, H. J. (2005). A little nip and tuck: axon refinement during development and axonal injury. Curr Opin Neurobiol *15*, 549-56.

LOW, L. K.; CHENG, H. J. (2006). Axon pruning: an essential step underlying the developmental plasticity of neuronal connections. Philos Trans R Soc Lond B Biol Sci *361*, 1531-44.

LUBKE, J. *et al.* (2003). Morphometric analysis of the columnar innervation domain of neurons connecting layer 4 and layer 2/3 of juvenile rat barrel cortex. Cereb Cortex *13*, 1051-63.

LUO, L.; O'LEARY, D. D. (2005). Axon retraction and degeneration in development and disease. Annu Rev Neurosci *28*, 127-56.

MAJEWSKA, A.; SUR, M. (2003). Motility of dendritic spines in visual cortex *in vivo*: changes during the critical period and effects of visual deprivation. Proc Natl Acad Sci U S A *100*, 16024-9.

MAJEWSKA, A. K. *et al.* (2006). Remodeling of synaptic structure in sensory cortical areas *in vivo*. J Neurosci *26*, 3021-9.

MARTIN, K. A. *et al.* (1983). Physiological and morphological properties of identified basket cells in the cat's visual cortex. Exp Brain Res *50*, 193-200.

MARTIN, K. A.; WHITTERIDGE, D. (1984). Form, function and intracortical projections of spiny neurones in the striate visual cortex of the cat. J Physiol *353*, 463-504.

MATAGA, N. *et al.* (2004). Experience-dependent pruning of dendritic spines in visual cortex by tissue plasminogen activator. Neuron *44*, 1031-41.

MCGUIRE, B. A. *et al.* (1991). Targets of horizontal connections in macaque primary visual cortex. J Comp Neurol *305*, 370-92.

MCKEE, S. P.; WESTHEIMER, G. (1978). Improvement in vernier acuity with practice. Percept Psychophys *24*, 258-62.

MERZENICH, M. M. *et al.* (1983). Topographic reorganization of somatosensory cortical areas 3b and 1 in adult monkeys following restricted deafferentation. Neuroscience *8*, 33-55.

MERZENICH, M. M. *et al.* (1983). Progression of change following median nerve section in the cortical representation of the hand in areas 3b and 1 in adult owl and squirrel monkeys. Neuroscience *10*, 639-65.

MERZENICH, M. M. *et al.* (1984). Somatosensory cortical map changes following digit amputation in adult monkeys. J Comp Neurol *224*, 591-605.

MINSKI, M. (1961). Microscopy apparatus. US patent 3013467.

MIZRAHI, A.; KATZ, L. C. (2003). Dendritic stability in the adult olfactory bulb. Nat Neurosci *6*, 1201-7.

NGUYEN, Q. T. *et al.* (2002). Pre-existing pathways promote precise projection patterns. Nat Neurosci *5*, 861-7.

NIELL, C. M. *et al*. (2004). *In vivo* imaging of synapse formation on a growing dendritic arbor. Nat Neurosci *7*, 254-260.

PAN, Y. A. *et al.* (2003). Effects of neurotoxic and neuroprotective agents on peripheral nerve regeneration assayed by time-lapse imaging *in vivo*. J Neurosci *23*, 11479-88.

PETERS, A. *et al.* (1991). The Fine Structure of the Nervous System: Neurons and Their Supporting Cells (New York: Oxford).

PETERS, A.; PROSKAUER, C. C. (1980). Synaptic relationships between a multipolar stellate cell and a pyramidal neuron in the rat visual cortex. A combined Golgi-electron microscope study. J Neurocytol *9*, 163-83.

PIERCE, J. P.; LEWIN, G. R. (1994). An ultrastructural size principle. Neuroscience *58*, 441-6.

POGGIO, T. *et al.* (1992). Fast perceptual learning in visual hyperacuity. Science *256*, 1018-21.

PONS, T. P. *et al.* (1991). Massive cortical reorganization after sensory deafferentation in adult macaques. Science *252*, 1857-60.

PORTERA-CAILLIAU, C. *et al.* (2005). Diverse modes of axon elaboration in the developing neocortex. PLoS Biol *3*, e272.

RAJAN, R. *et al.* (1993). Effect of unilateral partial cochlear lesions in adult cats on the representation of lesioned and unlesioned cochleas in primary auditory cortex. J Comp Neurol *338*, 17-49.

RAMACHANDRAN, V. S.; BRADDICK, O. (1973). Orientation-specific learning in stereopsis. Perception *2*, 371-6.

RECANZONE, G. H. *et al.* (1993). Plasticity in the frequency representation of primary auditory cortex following discrimination training in adult owl monkeys. J Neurosci *13*, 87-103.

ROBERTSON, D.; IRVINE, D. R. (1989). Plasticity of frequency organization in auditory cortex of guinea pigs with partial unilateral deafness. J Comp Neurol *282*, 456-71.

ROCKLAND, K. S.; LUND, J. S. (1982). Widespread periodic intrinsic connections in the tree shrew visual cortex. Science *215*, 1532-4.

ROCKLAND, K. S.; LUND, J. S. (1983). Intrinsic laminar lattice connections in primate visual cortex. J Comp Neurol *216*, 303-18.

ROELFSEMA, P. R. *et al.* (1998). Object-based attention in the primary visual cortex of the macaque monkey. Nature *395*, 376-81.

ROSE, J. E. *et al.* (1960). Effects of heavy, ionizing, monoenergetic particles on the cerebral cortex. II. Histological appearance of laminar lesions and growth of nerve fibers after laminar destructions. J Comp Neurol *115*, 243-55.

RUTHAZER, E. S. *et al.* (2003). Control of axon branch dynamics by correlated activity *in vivo*. Science *301*, 66-70.

RUTHAZER, E.S. *et al*. (2006). Stabilization of axon branch dynamics by synaptic maturation. J Neurosci *26*, 3594-3603.

SCHAEFER, A. M. *et al.* (2005). A compensatory subpopulation of motor neurons in a mouse model of amyotrophic lateral sclerosis. J Comp Neurol *490*, 209-19.

SCHIKORSKI, T.; STEVENS, C. F. (1997). Quantitative ultrastructural analysis of hippocampal excitatory synapses. J Neurosci *17*, 5858-67.

SCHIKORSKI, T.; STEVENS, C. F. (1999). Quantitative fine-structural analysis of olfactory cortical synapses. Proc Natl Acad Sci U S A *96*, 4107-12.

SCHMID, L. M. *et al.* (1996). Visuotopic reorganization in the primary visual cortex of adult cats following monocular and binocular retinal lesions. Cereb Cortex *6*, 388-405.

SCHMIDT, J. T. (2004). Activity-driven sharpening of the retinotectal projection: the search for retrograde synaptic signaling pathways. J Neurobiol *59*, 114-33.

SCHMIDT, J. T. *et al.* (2000). MK801 increases retinotectal arbor size in developing zebrafish without affecting kinetics of branch elimination and addition. J Neurobiol *42*, 303-14.

SCHOUPS, A. *et al.* (2001). Practising orientation identification improves orientation coding in V1 neurons. Nature *412*, 549-53.

SCHUCHARD, R. A. (1993). Validity and interpretation of Amsler grid reports. Arch Ophthalmol *111*, 776-80.

SCHUCHARD, R. A. (1995). Adaptation to macular scotomas in persons with low vision. Am J Occup Ther *49*, 870-6.

SCHUZ, A.; MUNSTER, A. (1985). Synaptic density on the axonal tree of a pyramidal cell in the cortex of the mouse. Neuroscience *15*, 33-9.

SHATZ, C. J.; STRYKER, M. P. (1978). Ocular dominance in layer IV of the cat's visual cortex and the effects of monocular deprivation. J Physiol *281*, 267-83.

SHIU, L. P.; PASHLER, H. (1992). Improvement in line orientation discrimination is retinally local but dependent on cognitive set. Percept Psychophys *52*, 582-8.

SIGMAN, M.; GILBERT, C. D. (2000). Learning to find a shape. Nat Neurosci *3*, 264-9.

SILVER, R. A. *et al.* (2003). High-probability uniquantal transmission at excitatory synapses in barrel cortex. Science *302*, 1981-4.

SMIRNAKIS, S. M. *et al.* (2005). Lack of long-term cortical reorganization after macaque retinal lesions. Nature *435*, 300-7.

SOMOGYI, P. (1978). The study of Golgi stained cells and of experimental degeneration under the electron microscope: a direct method for the identification in the visual cortex of three successive links in a neuron chain. Neuroscience *3*, 167-80.

SOMOGYI, P. *et al.* (1983). Retrograde transport of gamma-amino[3H]butyric acid reveals specific interlaminar connections in the striate cortex of monkey. Proc Natl Acad Sci U S A *80*, 2385-9.

SOMOGYI, P. *et al.* (1982). The axo-axonic interneuron in the cerebral cortex of the rat, cat and monkey. Neuroscience *7*, 2577-607.

STANFIELD, B. B. *et al.* (1982). Selective collateral elimination in early postnatal development restricts cortical distribution of rat pyramidal tract neurones. Nature *298*, 371-3.

STETTLER, D. D. *et al.* (2002). Lateral connectivity and contextual interactions in macaque primary visual cortex. Neuron *36*, 739-50.

STETTLER, D. D. *et al.* (2006). Axons and synaptic boutons are highly dynamic in adult visual cortex. Neuron *49*, 877-87.

SURACE, E. M. *et al.* (2003). Delivery of adeno-associated virus vectors to the fetal retina: impact of viral capsid proteins on retinal neuronal progenitor transduction. J Virol *77*, 7957-63.

SVOBODA, K. *et al.* (1997). *In vivo* dendritic calcium dynamics in neocortical pyramidal neurons. Nature *385*, 161-5.

TRACHTENBERG, J. T. *et al.* (2002). Long-term *in vivo* imaging of experience-dependent synaptic plasticity in adult cortex. Nature *420*, 788-94.

TRACHTENBERG, J. T.; STRYKER, M. P. (2001). Rapid anatomical plasticity of horizontal connections in the developing visual cortex. J Neurosci *21*, 3476-82.

TURNER, A. M.; GREENOUGH, W. T. (1985). Differential rearing effects on rat visual cortex synapses. I. Synaptic and neuronal density and synapses per neuron. Brain Res *329*, 195-203.

VOGELS, R.; ORBAN, G. A. (1985). The effect of practice on the oblique effect in line orientation judgments. Vision Res *25*, 1679-87.

VOLKMAR, F. R.; GREENOUGH, W. T. (1972). Rearing complexity affects branching of dendrites in the visual cortex of the rat. Science *176*, 1445-7.

WALSH, M. K.; LICHTMAN, J. W. (2003). *In vivo* time-lapse imaging of synaptic takeover associated with naturally occurring synapse elimination. Neuron *37*, 67-73.

WINFIELD, D. A. *et al.* (1981). A combined Golgi-electron microscopic study of the synapses made by the proximal axon and recurrent collaterals of a pyramidal cell in the somatic sensory cortex of the monkey. Neuroscience *6*, 1217-30.

WITTE, S. *et al.* (1996). *In vivo* observations of timecourse and distribution of morphological dynamics in Xenopus retinotectal axon arbors. J Neurobiol *31*, 219-34.

XIAO, W. *et al.* (1999). Gene therapy vectors based on adeno-associated virus type 1. J Virol *73*, 3994-4003.

YOSHIMURA, Y. *et al.* (2000). Properties of horizontal and vertical inputs to pyramidal cells in the superficial layers of the cat visual cortex. J Neurosci *20*, 1931-40.

YUSTE, R.; BONHOEFFER, T. (2004). Genesis of dendritic spines: insights from ultrastructural and imaging studies. Nat Rev Neurosci *5*, 24-34.

ZUO, Y. *et al.* (2005). Development of long-term dendritic spine stability in diverse regions of cerebral cortex. Neuron *46*, 181-9.

ZUR, D.; ULLMAN, S. (2003). Filling-in of retinal scotomas. Vision Res *43*, 971-82.